

On $B \rightarrow V\ell\ell$ at small dilepton invariant mass, power corrections, and new physics

S. JÄGER AND J. MARTIN CAMALICH

Department of Physics, University of Sussex, Brighton BN1 9QH, UK

Abstract

We investigate rare semileptonic $\bar{B} \rightarrow \bar{K}^*\ell^+\ell^-$ decays, providing a comprehensive treatment of theoretical uncertainties in the low- q^2 region as needed for interpreting current and future LHCb and B -factory data in terms of the new physics search. We go beyond the usual focus on form-factor uncertainties, paying proper attention to non-factorizable terms.

A central point is the systematic exploitation of the $V - A$ structure of SM weak interactions, which leads to the suppression of two helicity amplitudes and some of the angular coefficients. We review how this works at the level of (helicity) form factors, and show that the hierarchies extend to non-factorizable terms. For virtual charm effects, we give an argument for it in terms of light-cone QCD sum rules that continues to hold at the level of “long-distance” $\Lambda_{\text{QCD}}^2/m_c^2$ power corrections, reducing an important source of theoretical uncertainty in any $\bar{B}, \bar{B}_s \rightarrow V\ell^+\ell^-$ (or $\bar{B} \rightarrow V\gamma$) decay. The contributions of the remaining hadronic weak Hamiltonian respect a similar hierarchy. We employ a resonance model to preclude (in the $\bar{B} \rightarrow \bar{K}^*$ case) large long-distance corrections to this.

A phenomenological part pays particular attention to the region of lowest dilepton mass, $4m_\ell^2 \leq q^2 \leq 2 \text{ GeV}^2$. Two observables remain theoretically clean, implying a (theoretical) sensitivity to the real (imaginary) part of the “right-handed” Wilson coefficient C_7' to 10% (1%) of C_7^{SM} , both in the muonic and the electronic mode. We also show that there are two near-exact relations between angular coefficients, even in the presence of new physics and when lepton masses are not neglected.

1 Introduction

Rare B decays are CKM and/or loop-suppressed in the Standard Model (SM), which accounts for their small branching fractions and makes them sensitive to small contributions from possible new degrees of freedom beyond the SM (BSM). Unfortunately, they generally suffer from non-perturbative strong-interaction effects, the perennial bugbear of flavour (and collider) physics and difficult to control theoretically. An example where such uncertainties are small is provided by the decay $B_s \rightarrow \mu^+ \mu^-$, for which LHCb has just published first evidence [1],

$$BF(B_s \rightarrow \mu^+ \mu^-)_{\text{exp}} = (3.2_{-1.2}^{+1.4}|_{\text{stat}} \text{ }_{-0.3}^{+0.5}|_{\text{syst}}) \times 10^{-9} \quad [3.5\sigma \text{ significance}], \quad (1)$$

to be contrasted with the SM theory prediction,

$$BF(B_s \rightarrow \mu^+ \mu^-)_{\text{SM}} = (3.54 \pm 0.30) \times 10^{-9}, \quad (2)$$

which incorporates estimates of soft-photon emissions and takes account of the finite lifetime difference of the B_s [2, 3]. This result strongly constrains new-physics contributions through scalar \times scalar semileptonic operators, such as may occur in the MSSM at large $\tan \beta$. It also constrains physics entering through a modified Zbs vertex, although less strongly, and in view of the statistics foreseen at LHCb, this will remain so for the foreseeable future. Beyond this single, exceptionally clean example, one generally has to deal with amplitude ratios including strong rescattering phases, which are currently not tractable with a first-principles method like lattice QCD. One faces a trade-off between theoretical cleanness (as in leptonic decays) and number of modes, which increases with the number of hadrons in the final state, as does the theoretical complexity.

Rare semileptonic and radiative decays such as $\bar{B} \rightarrow \bar{K}^* \mu^+ \mu^-$ and $\bar{B} \rightarrow \bar{K}^* \gamma$ provide, in a sense, the best of both worlds. On the one hand, they have a rich kinematic and helicity structure. Experimental results on $\bar{B} \rightarrow \bar{K}^* \mu^+ \mu^-$ include measurements of the forward-backward asymmetry and the longitudinal polarisation fractions by the B -factories, CDF, and LHCb [4–7], of the angular observables $A_T^{(2)}$ and A_{im} by CDF [5, 8] and related angular coefficients by LHCb [6], and measurements of non-angular observables (e.g. [9–11]). Results on the full angular distribution are anticipated from LHCb. $\bar{B}_s \rightarrow \phi \mu^+ \mu^-$ has also been observed [12, 13]. On the theory side, there have been a large number of conceptual and phenomenological studies (e.g. [14–68]). On the other hand, involving only one hadron in the initial and final states, these modes approximately factorize naively, into products of nonperturbative form factors and Wilson coefficients given in terms of short-distance SM and BSM vertices. Naive factorization is, however, violated by the hadronic weak hamiltonian. Schematically,

$$\begin{aligned} \mathcal{A}(\bar{B} \rightarrow V \ell^- \ell^+) &= \sum_i C_i \langle \ell^- \ell^+ | \bar{l} \Gamma_i l | 0 \rangle \langle V | \bar{s} \Gamma'_i b | \bar{B} \rangle \\ &+ \frac{e^2}{q^2} \langle \ell^- \ell^+ | \bar{l} \gamma^\mu l | 0 \rangle F.T. \langle V | T \{ j_{\mu, \text{em}}^{\text{had}}(x) \mathcal{H}_{\text{eff}}^{\text{had}}(0) \} | \bar{B} \rangle, \quad (3) \end{aligned}$$

where C_i are semileptonic Wilson coefficients, $j_{\text{em}}^{\text{had}}$ is the hadronic part of the electromagnetic current, and $\mathcal{H}_{\text{eff}}^{\text{had}}$ is the hadronic weak $\Delta F = 1$ hamiltonian. This equation is correct up to higher orders in the QED coupling α_{em} . The form factors $\langle V | \bar{s} \Gamma'_i b | \bar{B} \rangle$ are, in principle, accessible on the lattice. For small dilepton invariant mass, they also lend themselves to light-cone sum rules [69], and satisfy certain constraints from heavy-quark symmetry/large-energy relations [70]. Making use of these relations, a number of observables can be shown to have reduced sensitivity to hadronic (form factor) uncertainties (see eg [15, 17, 32, 57]). However, this cleanness is compromised by the non-factorizable terms on the second line of (3), which pose the most challenging theoretical problem.

A breakthrough has been a comprehensive treatment of these effects within QCD factorization (QCDF) based on the heavy-quark limit [23, 24], valid for large hadronic recoil and in particular in the “low- q^2 ” region of dilepton invariant mass below the charmonium resonances, and for the radiative decay. At leading power in an expansion in Λ/m_b , where $\Lambda \equiv \Lambda_{\text{QCD}}$ is the dynamical QCD scale, the terms on the second line in (3) are expressed in terms of form factors, decay constants, and convolutions of light-cone distribution amplitudes of the initial and final state mesons with perturbative hard-scattering kernels. The same framework also allows one to systematically compute perturbative corrections to the form factor relations [71]. QCD factorization breaks at subleading powers, due to end-point divergences. The power corrections that do not factorize have to be modeled or constrained by some means, and those that do factorize are only partially known. Phenomenological analyses tend to either ignore power corrections or employ ad hoc estimates. On the other hand, a recent analysis [46] of power corrections within the framework of light-cone QCD sum rules (LCSR) found the possibility of large effects, of $\mathcal{O}(10\%)$ at the amplitude level. Importantly, some of the power corrections are of order $\Lambda^2/(4m_c^2)$, rather than Λ/m_b . All this is sufficient to cast into doubt the cleanness of the optimized observables.

In this paper, we revisit the issue of long-distance corrections, employing a systematic description in terms of helicity (as opposed to transversity) amplitudes. The point is that, when the treatment of [46] is reformulated in terms of helicity amplitudes, one can show a systematic suppression of the contributions of four-quark operators involving charm quarks to one (out of three) long-distance-sensitive helicity amplitudes, to be termed H_V^+ . This suppression in Λ/m_b holds even at the level of $\Lambda^2/(4m_c^2)$ power corrections. A suppression is likewise observed for the contributions of the chromomagnetic penguin operator Q_{8g} to H_V^+ . Moreover, if one adopts a resonance dominance model of long-distance contributions at low q^2 , one finds again a suppression of the amplitude in question. This eliminates the leading candidate of large “duality-violating” corrections to the QCDF results (and power-correction estimates) for the latter contributions.

The phenomenological relevance is as follows: Of the so-called “clean” observables, there are precisely two which vanish in the limit $H_V^+ \rightarrow 0$. These emerge as truly theoretically clean null tests of the Standard model, even with a conserva-

tive treatment of contributions from the hadronic weak Hamiltonian. Our results also show that this remains so at the $q^2 \rightarrow 0$ end of the dilepton invariant mass spectrum, which translates into good sensitivity to the “right-handed” magnetic Wilson coefficient C'_7 , as has been suggested earlier [72], even when fully taking account of hadronic effects. For the other observables, however, the new physics sensitivity becomes more limited.

The remainder of this paper is organised as follows. In Section 2 we set up our notation and review (and simplify) the decomposition of the decay amplitude and angular distribution, and “clean” observables, in helicity amplitudes. Section 3 contains a detailed discussion of sources of hadronic uncertainties both in the factorizable and non-factorizable contributions to the helicity amplitudes, and establishes the suppression of H_V^+ . We also employ a parameterization of form factors at low q^2 which transparently separates the constraints from kinematics and the heavy-quark limit from the issue of modelling power corrections. Section 4 comprises a detailed phenomenology of the “clean” observables, with particular attention to the low end of the low- q^2 region, which has traditionally been cut off ad hoc at $q^2 = 1 \text{ GeV}^2$. We find that the observables P_1 and P_3^{CP} (in the notation of [57]) in $\bar{B} \rightarrow \bar{K}^* \mu^+ \mu^-$ stand out as theoretically cleanest, translating to very good sensitivity to right-handed currents, via the Wilson coefficients C'_7 , C'_9 , and C'_{10} . Specifically, we assess the (theoretical) sensitivity to the real and imaginary parts of C'_7 to be on the order of 10% and 1%, respectively, with the sensitivity coming entirely from the region $q^2 < 3 \text{ GeV}^2$, and dominated by the q^2 -interval $[0.1, 2] \text{ GeV}^2$. We also comment on the electronic mode, which shows a theoretical sensitivity to C'_7 very similar to the muonic mode. Throughout we take into account both the small but nonzero values of right-handed Wilson coefficients in the SM and the effect of a nonzero muon mass, and show that two known algebraic relations in the massless case can be modified such that they hold, to excellent accuracy, in the presence of a finite muon mass all the way down to the kinematic end point. Section 5 contains our conclusions.

2 Amplitudes and kinematic distribution

2.1 Weak Hamiltonian

The process $\bar{B}(p) \rightarrow M(k)\ell^+\ell^-$, where M is a charmless final state (not necessarily a single meson), is mediated by the $\Delta B = 1$ weak effective Hamiltonian, which is a sum of hadronic and semileptonic parts (where “semileptonic” is understood to include the magnetic penguin terms),

$$\mathcal{H}_{\text{eff}} = \mathcal{H}_{\text{eff}}^{\text{had}} + \mathcal{H}_{\text{eff}}^{\text{sl}}, \quad (4)$$

with

$$\mathcal{H}_{\text{eff}}^{\text{had}} = \frac{4G_F}{\sqrt{2}} \sum_{p=u,c} \lambda_p \left[C_1 Q_1^p + C_2 Q_2^p + \sum_{i=3..6} C_i P_i + C_{8g} Q_{8g} \right], \quad (5)$$

$$\begin{aligned} \mathcal{H}_{\text{eff}}^{\text{sl}} = & -\frac{4G_F}{\sqrt{2}} \lambda_t \left[C_7 Q_{7\gamma} + C_7' Q_{7\gamma}' + C_9 Q_{9V} + C_9' Q_{9V}' + C_{10} Q_{10A} + C_{10}' Q_{10A}' \right. \\ & \left. + C_S Q_S + C_S' Q_S' + C_P Q_P + C_P' Q_P' + C_T Q_T + C_T' Q_T' \right]. \end{aligned} \quad (6)$$

The operators P_i are given in [73], the Q_i are defined as

$$\begin{aligned} Q_{7\gamma} &= \frac{e}{16\pi^2} \hat{m}_b \bar{s} \sigma_{\mu\nu} P_R F^{\mu\nu} b, & Q_{8g} &= \frac{g_s}{16\pi^2} \hat{m}_b \bar{s} \sigma_{\mu\nu} P_R G^{\mu\nu} b, \\ Q_{9V} &= \frac{\alpha_{\text{em}}}{4\pi} (\bar{s} \gamma_\mu P_L b) (\bar{l} \gamma^\mu l), & Q_{10A} &= \frac{\alpha_{\text{em}}}{4\pi} (\bar{s} \gamma_\mu P_L b) (\bar{l} \gamma^\mu \gamma^5 l)_A, \\ Q_S &= \frac{\alpha_{\text{em}}}{4\pi} \frac{\hat{m}_b}{m_W} (\bar{s} P_R b) (\bar{l} l), & Q_P &= \frac{\alpha_{\text{em}}}{4\pi} \frac{\hat{m}_b}{m_W} (\bar{s} P_R b) (\bar{l} \gamma^5 l), \\ Q_T &= \frac{\alpha_{\text{em}}}{4\pi} \frac{\hat{m}_b}{m_W} (\bar{s} \sigma_{\mu\nu} P_R b) (\bar{l} \sigma^{\mu\nu} P_R l), \end{aligned} \quad (7)$$

and the primed operators Q_i' are obtained from these by $P_R \rightarrow P_L, P_L \rightarrow P_R$ in the quark bilinears. g_s (e) denotes the strong (electromagnetic) coupling constant coming from the covariant derivative $D_\mu = \partial_\mu + ieQ_f A_\mu + ig_s T^A A_\mu^A$ ($Q_f = -1$ for the leptons), $\alpha_{\text{em}} = e^2/(4\pi)$ and \hat{m}_b the b -quark mass defined in the $\overline{\text{MS}}$ scheme.

The contribution of the semileptonic Hamiltonian $\mathcal{H}_{\text{eff}}^{\text{sl}}$ to the decay amplitude factorizes (in the ‘‘naive’’ sense) into a sum of products of hadronic and leptonic currents,

$$\mathcal{A}^{\text{sl}} = \langle M \ell^+ \ell^- | \mathcal{H}_{\text{eff}}^{\text{sl}} | \bar{B} \rangle = L_V^\mu a_{V\mu} + L_A^\mu a_{A\mu} + L_S a_S + L_P a_P + L_{TL}^\mu a_{TL,\mu} + L_{TR}^\mu a_{TR,\mu}, \quad (8)$$

where

$$\begin{aligned} L_V^\mu &= \langle \ell^+ \ell^- | \bar{l} \gamma^\mu l | 0 \rangle, & L_A^\mu &= \langle \ell^+ \ell^- | \bar{l} \gamma^\mu \gamma^5 l | 0 \rangle, \\ L_S &= \langle \ell^+ \ell^- | \bar{l} l | 0 \rangle, & L_P &= \langle \ell^+ \ell^- | \bar{l} \gamma^5 l | 0 \rangle, \\ L_{TL}^\mu &= \frac{i}{\sqrt{q^2}} \langle \ell^+ \ell^- | q_\nu \bar{l} \sigma^{\mu\nu} P_L l | 0 \rangle, & L_{TR}^\mu &= \frac{i}{\sqrt{q^2}} \langle \ell^+ \ell^- | q_\nu \bar{l} \sigma^{\mu\nu} P_R l | 0 \rangle, \end{aligned} \quad (9)$$

and we have made use of the relation

$$(\bar{s} \sigma_{\mu\nu} P_{R(L)} b) (\bar{l} \sigma^{\mu\nu} P_{R(L)} s) = \frac{4}{q^2} (\bar{s} q_\nu \sigma^{\mu\nu} P_{R(L)} b) (\bar{l} q_\rho \sigma^{\mu\rho} P_{R(L)} l), \quad (10)$$

where $q = p - k$ is the dilepton four-momentum.¹ The hadronic currents $a_{V\mu}, \dots$ are expressed in terms of form factors and Wilson coefficients, and enter the helicity amplitudes given below.

¹Equation (10) holds for arbitrary time-like four-vector q_μ .

The hadronic Hamiltonian \mathcal{H}_{eff} requires in addition two insertions of the electromagnetic current (one hadronic and one leptonic) to mediate the semileptonic decay,

$$\begin{aligned} \mathcal{A}^{(\text{had})} &= -i \frac{e^2}{q^2} \int d^4x e^{-iq \cdot x} \langle \ell^+ \ell^- | j_\mu^{\text{em,lept}}(x) | 0 \rangle \int d^4y e^{iq \cdot y} \langle M | T \{ j^{\text{em,had},\mu}(y) \mathcal{H}_{\text{eff}}^{\text{had}}(0) \} | \bar{B} \rangle \\ &\equiv \frac{e^2}{q^2} L_V^\mu a_\mu^{\text{had}} \ , \end{aligned} \tag{11}$$

where $j^{\text{em,had},\mu} = \sum_q e_q \bar{q} \gamma^\mu q$. Hence, while this contribution does not naively factorize, it can be absorbed into $a_{V\mu}$ in (8). Before discussing the amplitudes in more detail, we comment on the approximations implicit in and some consequences of (8), (11)

- The semileptonic weak Hamiltonian is the most general one up to dimension six and can accommodate arbitrary new physics with a heavy mass scale. This includes all the standard scenarios, such as supersymmetry, extra dimensions and little Higgs. In the Standard Model, C_7 , C_9 and C_{10} are sizable, C_7' is suppressed by m_s/m_b , and the remaining Wilson coefficients are negligible.
- The hadronic weak Hamiltonian is the Standard Model one, neglecting the small electroweak penguin terms. Beyond the Standard Model, there is a large number of extra operators; however unless new physics effects are dramatic their impact (through a_μ^{had}) will be very small and we will ignore them below. Such scenarios are also constrained by hadronic B decay data.
- We work to leading order in the electromagnetic coupling, but all formulae so far are exact in the strong coupling, with non-factorizable effects confined to a_μ^{had} .
- The leptonic currents can be decomposed into spin-0 and spin-1 terms (L_V^μ , L_A^μ) or are pure spin-1 objects (L_{TL}^μ , L_{TR}^μ). It follows that the dilepton can only be created in a spin-0 or spin-1 state. Angular momentum conservation then implies that λ is also the helicity of M , which is thus constrained to the values ± 1 or 0 even if M has spin greater than one.²

² This statement is exact, rather than a consequence of naive factorization, following from the well-known fact that a particle's orbital angular momentum does not contribute to its helicity. If M is a multiparticle state, eg $K\pi$, we mean by "spin" the total angular momentum of M in its cm frame and by "helicity" the projection of the M angular momentum onto the total M momentum in the \bar{B} rest frame.

2.2 Helicity amplitudes and helicity form factors

We now carry out the decomposition of the leptonic currents in spins and helicities. The resulting coefficients give the well-known ‘‘helicity amplitudes’’ [16]. This is easily achieved [39] through the completeness relation (see Appendix A.1 for our conventions)

$$\eta_{\mu\nu} = \epsilon_{t,\mu}\epsilon_{t,\nu}^* - \sum_{\lambda=\pm 1,0} \epsilon_{\mu}(1,\lambda)\epsilon_{\nu}^*(1,\lambda). \quad (12)$$

Here $\epsilon(1,\lambda)$, $\lambda = \pm 1, 0$, denotes a (spin-1) helicity triplet of polarisation 4-vectors for a vector particle of four-momentum q^μ and mass $\sqrt{q^2}$, and $\epsilon_t^\mu = q^\mu/\sqrt{q^2}$. We may picture the latter as the ‘‘time-like’’ polarization four-vector of an auxiliary virtual gauge boson of mass $\sqrt{q^2}$, but the decomposition works independently of the origin of the weak Hamiltonian, and also for the tensorial currents. The result is

$$\begin{aligned} \mathcal{A} = & - \sum_{\lambda=\pm 1,0} \mathcal{L}_V(\lambda)H_V(\lambda) - \sum_{\lambda=\pm 1,0} \mathcal{L}_A(\lambda)H_A(\lambda) + L_S H_S + L_P H_P \\ & - \sum_{\lambda=\pm 1,0} \mathcal{L}_{TL}(\lambda)H_{TL}(\lambda) - \sum_{\lambda=\pm 1,0} \mathcal{L}_{TR}(\lambda)H_{TR}(\lambda), \end{aligned} \quad (13)$$

where

$$\begin{aligned} \mathcal{L}_V(\lambda) &= \epsilon_{\mu}(\lambda)L_V^\mu, & H_V(\lambda) &= \epsilon_{\mu}^*(\lambda)a_V^\mu, \\ \mathcal{L}_A(\lambda) &= \epsilon_{\mu}(\lambda)L_A^\mu, & H_A(\lambda) &= \epsilon_{\mu}^*(\lambda)a_A^\mu, \\ \mathcal{L}_{TL}(\lambda) &= \epsilon_{\mu}(\lambda)L_{TL}^\mu, & H_{TL}(\lambda) &= \epsilon_{\mu}^*(\lambda)a_{TL}^\mu, \\ \mathcal{L}_{TR}(\lambda) &= \epsilon_{\mu}(\lambda)L_{TR}^\mu, & H_{TR}(\lambda) &= \epsilon_{\mu}^*(\lambda)a_{TR}^\mu, \\ \mathcal{L}_S &= L_S, & H_S &= a_S \\ \mathcal{L}_P &= L_P, & H_P &= a_P + \frac{2m_\ell}{q^2}q_\mu a_A^\mu. \end{aligned} \quad (14)$$

We have made use of the fact that all leptonic currents except for L_A^μ are conserved, so $\epsilon_{t,\mu}$ contracts to zero with them. Moreover, the axial current obeys $q_\mu L_A^\mu = 2m_\ell L_P$, which allowed us to absorb the spin-zero axial vector amplitude into H_P [39].³

The helicity amplitudes H_V, H_A, H_P, H_S are related to the ‘‘standard’’ helicity amplitudes [18, 39] as follows,

$$H_{\lambda L/R} = i\sqrt{f}\frac{1}{2}(H_V(\lambda) \mp H_A(\lambda)), \quad A_t = i\frac{\sqrt{q^2}}{2m_\ell}\sqrt{f}H_P, \quad A_S = -i\sqrt{f}H_S, \quad (15)$$

³We do not distinguish between the lepton mass m_ℓ and the lepton field mass parameter, as we will work to leading order in the electromagnetic coupling.

where f is a normalization factor, which for $M = K^*$ and the conventions of [39] is equal to F defined in Section 2.3 below. The helicity amplitudes $H_{\pm 1, L(R)}$ are often expressed in terms of transversity amplitudes,

$$A_{\parallel L(R)} = \frac{1}{\sqrt{2}}(H_{+1, L(R)} + H_{-1, L(R)}), \quad A_{\perp L(R)} = \frac{1}{\sqrt{2}}(H_{+1, L(R)} - H_{-1, L(R)}). \quad (16)$$

However, we will work with helicity amplitudes throughout this paper, for reasons to become clear below. Explicitly, we have

$$H_V(\lambda) = -i N \left\{ C_9 \tilde{V}_{L\lambda} + C_9' \tilde{V}_{R\lambda} + \frac{m_B^2}{q^2} \left[\frac{2\hat{m}_b}{m_B} (C_7 \tilde{T}_{L\lambda} + C_7' \tilde{T}_{R\lambda}) - 16\pi^2 h_\lambda \right] \right\}, \quad (17)$$

$$H_A(\lambda) = -i N (C_{10} \tilde{V}_{L\lambda} + C_{10}' \tilde{V}_{R\lambda}), \quad (18)$$

$$H_{TR}(\lambda) = -i N \frac{4\hat{m}_b m_B}{m_W \sqrt{q^2}} C_T \tilde{T}_{L\lambda}, \quad (19)$$

$$H_{TL}(\lambda) = -i N \frac{4\hat{m}_b m_B}{m_W \sqrt{q^2}} C_T' \tilde{T}_{R\lambda}, \quad (20)$$

$$H_S = i N \frac{\hat{m}_b}{m_W} (C_S \tilde{S}_L + C_S' \tilde{S}_R), \quad (21)$$

$$H_P = i N \left\{ \frac{\hat{m}_b}{m_W} (C_P \tilde{S}_L + C_P' \tilde{S}_R) + \frac{2m_\ell \hat{m}_b}{q^2} \left[C_{10} \left(\tilde{S}_L - \frac{m_s}{m_b} \tilde{S}_R \right) + C_{10}' \left(\tilde{S}_R - \frac{m_s}{m_b} \tilde{S}_L \right) \right] \right\}, \quad (22)$$

where

$$N = -\frac{4G_F m_B}{\sqrt{2}} \frac{e^2}{16\pi^2} \lambda_t$$

is a normalisation factor,

$$h_\lambda \equiv \frac{i}{m_B^2} \epsilon^{\mu*}(\lambda) a_\mu^{\text{had}} \quad (23)$$

contains the contribution from the hadronic hamiltonian, i.e. all non-factorizable effects, and we have defined helicity form factors

$$-im_B \tilde{V}_{L(R)\lambda}(q^2) = \langle M(\lambda) | \bar{s} \not{\epsilon}^*(\lambda) P_{L(R)} b | \bar{B} \rangle, \quad (24)$$

$$m_B^2 \tilde{T}_{L(R)\lambda}(q^2) = \epsilon^{*\mu}(\lambda) q^\nu \langle M(\lambda) | \bar{s} \sigma_{\mu\nu} P_{R(L)} b | \bar{B} \rangle, \quad (25)$$

$$im_B \tilde{S}_{L(R)}(q^2) = \langle M(\lambda = 0) | \bar{s} P_{R(L)} b | \bar{B} \rangle. \quad (26)$$

These expressions are still general enough to describe an arbitrary charmless final state M . Concretely, for a two-spinless-meson final state, not necessarily originating from a resonance, the form factors will carry dependence on the dimeson invariant mass k^2 and its angular momentum L , in addition to the dilepton invariant mass q^2 .

Note that parity invariance of strong interactions implies the relations

$$\tilde{V}_{L\lambda} = -\eta(-1)^L \tilde{V}_{R,-\lambda} \equiv \tilde{V}_\lambda, \quad (27)$$

$$\tilde{T}_{L\lambda} = -\eta(-1)^L \tilde{T}_{R,-\lambda} \equiv \tilde{T}_\lambda, \quad (28)$$

$$\tilde{S}_L = -\eta(-1)^L \tilde{S}_R \equiv \tilde{S}, \quad (29)$$

where s and η are (respectively) the angular momentum and intrinsic parity of M . For a resonance, its spin s replaces L . Hence there are seven independent helicity form factors for $\text{spin} \geq 1$ and three for $\text{spin} = 0$ (when $\lambda = 0$). Helicity form factors have previously been used in the literature as a technical vehicle in constraining form factors from unitarity [74]. As we will explain in detail below, helicity form factors are also preferable over the standard basis for form factors in weak decays: Not only do they simplify the expressions, but some of them are systematically suppressed, which can and should be exploited to reduce important sources of uncertainty.

We also find it convenient to define rescaled helicity-0 form factors as

$$\begin{aligned} V_0(q^2) &= \frac{2m_B \sqrt{q^2}}{\lambda^{1/2}} \tilde{V}_0(q^2), \\ T_0(q^2) &= \frac{2m_B^3}{\sqrt{q^2} \lambda^{1/2}} \tilde{T}_0(q^2), \\ S(q^2) &= -\frac{2m_B(m_b + m_s)}{\lambda^{1/2}} \tilde{S}(q^2), \end{aligned} \quad (30)$$

where $\lambda = 4m_B^2 |\vec{k}|^2$ (\vec{k} is the 3-momentum of the recoiling meson in the \bar{B} rest frame), and also define $V_{\pm 1}(q^2) \equiv \tilde{V}_{\pm 1}(q^2)$, $T_{\pm 1}(q^2) \equiv \tilde{T}_{\pm 1}(q^2)$. The helicity form factors can be expressed in terms of the traditional form factors. For a vector, we then have (conventions for polarisation vectors and form factors in Appendix A)

$$\begin{aligned} V_{\pm}(q^2) &= \frac{1}{2} \left[\left(1 + \frac{m_V}{m_B} \right) A_1(q^2) \mp \frac{\lambda^{1/2}}{m_B(m_B + m_V)} V(q^2) \right], \\ V_0(q^2) &= \frac{1}{2m_V \lambda^{1/2} (m_B + m_V)} \left[(m_B + m_V)^2 (m_B^2 - q^2 - m_V^2) A_1(q^2) - \lambda A_2(q^2) \right], \\ T_{\pm}(q^2) &= \frac{m_B^2 - m_V^2}{2m_B^2} T_2(q^2) \mp \frac{\lambda^{1/2}}{2m_B^2} T_1(q^2), \\ T_0(q^2) &= \frac{m_B}{2m_V \lambda^{1/2}} \left[(m_B^2 + 3m_V^2 - q^2) T_2(q^2) - \frac{\lambda}{(m_B^2 - m_V^2)} T_3(q^2) \right], \\ S(q^2) &= A_0(q^2), \end{aligned} \quad (31)$$

We also have $V_{R\lambda} = -V_{-\lambda}$, $T_{R\lambda} = -T_{-\lambda}$, $S_R = -S_L$.

For a pseudoscalar, we have

$$V_0(q^2) = if_+(q^2), \quad (32)$$

$$T_0(q^2) = i \frac{2m_B}{(m_B + m_P)} f_T(q^2), \quad (33)$$

$$S(q^2) = \frac{1 + \frac{m_s}{m_b} m_B^2 - m_M^2}{1 - \frac{m_s}{m_b}} \frac{1}{\lambda^{1/2}} f_0(q^2). \quad (34)$$

In this case, $V_{R0} = V_0$, $T_{R0} = T_0$, $S_R = S$.

2.3 Kinematic distribution

We now consider the process

$$\bar{B}(p) \rightarrow V(k) [\rightarrow \bar{K}(k_1) \pi(k_2)] \ell^-(q_1) \ell^+(q_2), \quad (35)$$

i.e. decays to a vector decaying further into two pseudoscalars (for definiteness, a kaon and a pion, with $\bar{K} = \bar{K}^0$ or K^- , $\pi = \pi^+$ or π^0), where all four final-state particles carry definite four-momenta. These are the states in which detection is made. Following [32], we define angles θ_K, θ_l, ϕ as follows. We first define, in the \bar{B} rest frame,

$$\mathbf{e}_l = \frac{\mathbf{p}_{l^-} \times \mathbf{p}_{l^+}}{|\mathbf{p}_{l^-} \times \mathbf{p}_{l^+}|}, \quad \mathbf{e}_K = \frac{\mathbf{p}_{\bar{K}} \times \mathbf{p}_\pi}{|\mathbf{p}_{\bar{K}} \times \mathbf{p}_\pi|}, \quad \hat{z} = \frac{\mathbf{p}_{\bar{K}} + \mathbf{p}_\pi}{|\mathbf{p}_{\bar{K}} + \mathbf{p}_\pi|}. \quad (36)$$

Then define ϕ , in the interval $[0, 2\pi]$, through $\sin \phi = (\mathbf{e}_l \times \mathbf{e}_K) \cdot \hat{z}$ and $\cos \phi = \mathbf{e}_l \cdot \mathbf{e}_K$. Moreover, θ_l is defined as the angle between the direction of flight of the \bar{B} and the ℓ^- in the dilepton rest frame and θ_K as the angle between the direction of motion of the \bar{B} and the \bar{K} in the dimeson (\bar{K}^*) rest frame, both in the interval $[0, \pi)$. For a B decay, we define the angles in the same way, in particular θ_l is the angle between the ℓ^- (rather than the ℓ^+) and the B . This convention agrees with [39] and leads to simple expressions for untagged observables.

Next, we assume a resonant decay through an on-shell vector meson. (This means we are making a narrow-width approximation.⁴) We should then make the replacement

$$|\bar{K}^*; \lambda\rangle \longrightarrow \sqrt{b} \int d\Omega_K Y_1^\lambda(\theta, \phi_K) |\theta_K; \phi_K\rangle, \quad (37)$$

where θ_K is the angle between the $+z$ direction and the \bar{K} direction in the \bar{K}^* cm frame and ϕ_K is the angle between the x axis and the projection of the

⁴ Off-resonance effects vanish in the limit of an infinitely narrow \bar{K}^* . They can be included in the framework by introducing dependence on the hadronic final state invariant mass k^2 and total angular momentum L in the helicity amplitudes [55]. In particular, off-resonant $L = 0$ (S -wave) contributions have been recently studied in [58, 61, 62]. They modify some of the angular coefficients, but do not impact on those that involve only $\lambda = \pm 1$ amplitudes.

former onto the xy plane, and $b \equiv BF(K^* \rightarrow K\pi) \approx 1$. (Except for the zero point of the angle ϕ_K , this is entirely fixed by conservation of probability and of angular momentum and is independent of the details of the \bar{K}^* decay vertex. See also [55].) Squaring the amplitude and summing over lepton spins the fully differential decay rate is obtained as

$$\begin{aligned} \frac{d^{(4)}\Gamma}{dq^2 d(\cos\theta_l)d(\cos\theta_k)d\phi} &= \frac{9}{32\pi} \\ &\times \left(I_1^s \sin^2\theta_k + I_1^c \cos^2\theta_k + (I_2^s \sin^2\theta_k + I_2^c \cos^2\theta_k) \cos 2\theta_l \right. \\ &+ I_3 \sin^2\theta_k \sin^2\theta_l \cos 2\phi + I_4 \sin 2\theta_k \sin 2\theta_l \cos \phi \\ &+ I_5 \sin 2\theta_k \sin \theta_l \cos \phi + (I_6^s \sin^2\theta_k + I_6^c \cos^2\theta_k) \cos \theta_l \\ &\left. + I_7 \sin 2\theta_k \sin \theta_l \sin \phi + I_8 \sin 2\theta_k \sin 2\theta_l \sin \phi + I_9 \sin^2\theta_k \sin^2\theta_l \sin 2\phi \right). \end{aligned} \quad (38)$$

The angular coefficients I_i are functions exclusively of q^2 . They can be expressed in terms of the helicity or transversity amplitudes Eqs. (17)–(22) as

$$\begin{aligned} I_1^c &= F \left\{ \frac{1}{2} (|H_V^0|^2 + |H_A^0|^2) + |H_P|^2 + \frac{2m_\ell^2}{q^2} (|H_V^0|^2 - |H_A^0|^2) + \beta^2 |H_S|^2 \right\}, \\ I_1^s &= F \left\{ \frac{\beta^2 + 2}{8} (|H_V^+|^2 + |H_V^-|^2 + (V \rightarrow A)) + \frac{m_\ell^2}{q^2} (|H_V^+|^2 + |H_V^-|^2 - (V \rightarrow A)) \right\}, \\ I_2^c &= -F \frac{\beta^2}{2} (|H_V^0|^2 + |H_A^0|^2), \\ I_2^s &= F \frac{\beta^2}{8} (|H_V^+|^2 + |H_V^-|^2) + (V \rightarrow A), \\ I_3 &= -\frac{F}{2} \text{Re} [H_V^+ (H_V^-)^*] + (V \rightarrow A), \\ I_4 &= F \frac{\beta^2}{4} \text{Re} [(H_V^- + H_V^+) (H_V^0)^*] + (V \rightarrow A), \\ I_5 &= F \left\{ \frac{\beta}{2} \text{Re} [(H_V^- - H_V^+) (H_A^0)^*] + (V \leftrightarrow A) - \frac{\beta m_\ell}{\sqrt{q^2}} \text{Re} [H_S^* (H_V^+ + H_V^-)] \right\}, \\ I_6^s &= F\beta \text{Re} [H_V^- (H_A^-)^* - H_V^+ (H_A^+)^*], \\ I_6^c &= 2F \frac{\beta m_\ell}{\sqrt{q^2}} \text{Re} [H_S^* H_V^0], \\ I_7 &= F \left\{ \frac{\beta}{2} \text{Im} [(H_A^+ + H_A^-) (H_V^0)^*] + (V \leftrightarrow A) - \frac{\beta m_\ell}{\sqrt{q^2}} \text{Im} [H_S^* (H_V^- - H_V^+)] \right\}, \\ I_8 &= F \frac{\beta^2}{4} \text{Im} [(H_V^- - H_V^+) (H_V^0)^*] + (V \rightarrow A), \\ I_9 &= F \frac{\beta^2}{2} \text{Im} [H_V^+ (H_V^-)^*] + (V \rightarrow A), \end{aligned} \quad (39)$$

where

$$F = \frac{\lambda^{1/2} \beta q^2}{3 \times 2^5 \pi^3 m_B^3} BF(K^* \rightarrow K\pi), \quad \beta = \sqrt{1 - \frac{4m_\ell^2}{q^2}}.$$

We have omitted the terms involving the tensor amplitudes H_{TL} and H_{TR} , which will be considered elsewhere. The phenomenology in Section 4 will be incomplete in this sense, but as explained there, we expect the effect on the considered observables to be very small.

The analysis of the CP-partner decay $B \rightarrow K^* \mu^+ \mu^-$ gives rise to an equivalent distribution, $d^{(4)}\bar{\Gamma}/(dq^2 d(\cos\theta_l)d(\cos\theta_k)d\phi)$, which is obtained from (38) by replacing

$$I_{1s(c),2s(c),3,4,7} \rightarrow \bar{I}_{1s(c),2s(c),3,4,7}, \quad \bar{I}_{5,6,8,9} \rightarrow -\bar{I}_{5,6,8,9}, \quad (40)$$

when one uses the angles defined as in the \bar{B} decays with $K^- \rightarrow K^+$ [18]. In the later equation the \bar{I}_i 's are equal to the I_i 's but with all the weak phases conjugated.

2.4 “Clean” observables, helicity hierarchies, and new physics

The 12 angular coefficients, together with their CP-conjugates, provide complete information about the decay distribution. In practice, however, certain combinations of these observables are more useful. Two important examples are the forward-backward asymmetry [14, 15, 17] and the transverse asymmetry $A_T^{(2)}$ [32],

$$A_{FB}(q^2) \equiv \frac{\left[\int_0^1 - \int_{-1}^0 \right] d(\cos\theta_l) d^2\Gamma' / (dq^2 d\cos\theta_l)}{\int_{-1}^1 d(\cos\theta_l) d^2\Gamma' / (dq^2 d\cos\theta_l)} = -\frac{3\Sigma_6^s}{4\Gamma'}, \quad (41)$$

$$A_T^{(2)} \equiv \frac{\Sigma_3}{2\Sigma_{2s}} \equiv P_1, \quad (42)$$

where $\Sigma_i \equiv (I_i + \bar{I}_i)/2$ and $d\Gamma' = (d\Gamma + d\bar{\Gamma})/2$ denote CP-averages. These have two potential advantages. First, taking ratios leads to cancellations of form factor uncertainties between the numerator and denominator. In particular, P_1 only involves the amplitudes H_V^\pm and H_A^\pm . In the factorizable approximation and neglecting the small Wilson coefficients C'_7 , C'_9 , and C'_{10} , this leaves dependence only on T_- , V_- , T_+ , and V_+ . For energetic $E_V \sim m_b$ (small q^2), one has the heavy-quark/large-energy relations $T_- = V_-$, $T_+ = V_+ = 0$ (see below), which are broken only by (calculable) α_s -corrections and (incalculable) Λ/m_b power corrections. Neglecting these, too, the single remaining form factor then cancels out between the numerator and denominator. In the case of A_{FB} , the cancellation is incomplete, as the denominator involves further amplitudes. However, the location of the zero-crossing q_0^2 is determined entirely by the numerator, and (under the same approximations) is free of form factor uncertainties. For these

reasons, P_1 , q_0^2 , and similar observables are often termed “clean”. An optimized set has been recently defined in [57] and will be studied in the phenomenological part below.

A second point is that P_1 actually vanishes under the stated approximations, as a consequence of all terms being proportional to either V_+ or T_+ . Hence, it is an approximate null-test of the Standard Model, and a probe of any new physics that generates the Wilson coefficients C'_7 , C'_9 , or C'_{10} . The same is true of I_9 and certain combinations constructed from it.

Clearly, the actual theoretical cleanness of the observables will depend on the size of the radiative and power corrections and non-factorizable effects. The following section is devoted to a thorough study of these effects, and their impact on the “wrong-helicity” amplitudes H_V^+ and H_A^+ in particular. We will show that, under very conservative assumptions, H_V^+ and H_A^+ remain suppressed, such that the clean character of I_3 and I_9 as null tests, but not of other observables, is preserved by non-factorizable and power corrections.

Finally, let us recall that the radiative decay $\bar{B} \rightarrow V\gamma$ is described in terms of a subset of the amplitudes for $\bar{B} \rightarrow V\ell^+\ell^-$. The precise relation is ($\lambda = \pm 1$)

$$\begin{aligned} \mathcal{A}(\bar{B} \rightarrow V(\lambda)\gamma(\lambda)) &= \lim_{q^2 \rightarrow 0} \frac{q^2}{e} H_V(q^2 = 0; \lambda) \\ &= \frac{iNm_B^2}{e} \left[\frac{2\hat{m}_b}{m_B} (C_7\tilde{T}_\lambda(0) - C'_7\tilde{T}_{-\lambda}(0) - 16\pi^2 h_\lambda(q^2 = 0)) \right]. \end{aligned} \tag{43}$$

3 Helicity amplitudes: anatomy, hierarchies, and hadronic uncertainties

The helicity amplitudes governing the observables involve form factors and the nonlocal objects h_λ , all of which carry hadronic uncertainties, limiting the sensitivity of rare B decays to new physics. However, hadronic uncertainties can be constrained by means of the equations of motion, the $V - A$ structure of the weak hamiltonian, and an expansion in Λ/m_b (QCD factorization). Our main point is that this results in the suppression of entire helicity amplitudes, including non-factorizable effects, such that the discussion is indeed best framed in terms of helicity (rather than transversity) amplitudes and helicity form factors. We first translate what is known about the form factors to the helicity basis, including the fact that the heavy-quark limit implies the suppression of two of them [20]. We next survey how this bears out in various theoretical approaches to form factor determinations, concluding with a brief argument for the suppression of the positive-helicity form factors in the framework of light-cone sum rules, at the level of the correlation function. We then show that the $V - A$ structure also implies

suppression of the “charm-loop” contribution to the nonlocal positive-helicity amplitude h_{+1} , building on a method introduced in [46]. In addition, we show that the same conclusion applies to hadronic resonance models for the “light-quark” contributions to h_λ , once known experimental facts about the helicity structure of $\bar{B} \rightarrow VV$ are incorporated (which can be theoretically understood on the same basis).

3.1 Form factors

The $\bar{B} \rightarrow M$ form factors are nonperturbative objects. In the following, we restrict ourselves to the $\bar{B} \rightarrow V$ case. First-principles lattice-QCD computations are becoming available [75,76], although they will be restricted for the foreseeable future to the region of slow-moving V (high q^2). A state-of-the-art method of obtaining form factors at low q^2 is given by QCD sum rules on the light cone (see [69, 77]). This involves, unfortunately, certain irreducible systematic uncertainties which are difficult to quantify. Sum rules are also useful in guiding extrapolations of high- q^2 lattice-QCD results [74].

3.1.1 Theoretical constraints on form factors at low q^2

The form factors fulfil two exact relations that in the helicity basis take the form

$$T_+(q^2 = 0) = 0, \tag{44}$$

$$S(q^2 = 0) = V_0(0). \tag{45}$$

At large recoil, i.e. small q^2 , one has further relations which hold up to corrections of $\mathcal{O}(\Lambda/m_b)$ but to all orders in α_s . As a result, the seven form factors are given, at leading power in Λ/m_b and Λ/E (where $E \equiv E_V$ is itself of order m_b for low q^2), in terms of only two independent *soft* form factors [70], ξ_\perp and ξ_\parallel , with radiative corrections systematically calculable in QCDF [71] as a perturbative expansion in α_s . These corrections also involve nonperturbative objects such as decay constants and light-cone distribution amplitudes (LCDAs) of the initial and final mesons. The factorization properties and calculation of radiative corrections become particularly transparent when formulated as a matching of QCD to soft-collinear effective theory (SCET) [78–81]. Corrections at $\mathcal{O}(\Lambda/m_b)$ violate factorization and need to be modeled, or estimated or constrained by another method.

The soft form factors can be chosen to coincide with two “physical”, i.e. full-QCD form factors, which makes them well-defined to all orders in Λ/m_b . Appropriate choices are V and A_0 , for ξ_\perp and ξ_\parallel respectively [71], given that they are matrix elements of conserved currents and, as such, free from renormalization scale ambiguities. For ξ_\perp , we find it convenient to use the transversity form factor T_1 instead. In this case, however, the transversal soft form factor depends on the

factorization scale μ as (to LL accuracy)

$$T_1(q^2, \mu) \equiv \xi_\perp(q^2, \mu) = \xi_\perp(q^2, m_b) \left(\frac{\alpha_s(\mu)}{\alpha_s(m_b)} \right)^{4/23}. \quad (46)$$

Setting

$$\begin{aligned} T_1(q^2, \mu) &\equiv \xi_\perp(q^2, \mu), \\ S(q^2) &\equiv \frac{E}{m_V} \xi_\parallel(q^2), \end{aligned}$$

with $E \simeq (m_B^2 - q^2)/(2m_B)$, the symmetry relations in Ref. [71] can be expressed in the helicity basis as

$$\begin{aligned} T_- &= \frac{2E}{m_B} \xi_\perp, \\ T_+ &= 0, \\ T_0 &= \frac{E}{m_V} \xi_\parallel \left(1 + \frac{\alpha_s C_F}{4\pi} \left[\ln \frac{m_b^2}{\mu^2} - 2 + 4L \right] \right) + \frac{\alpha_s C_F}{4\pi} \Delta T_0, \\ V_- &= \frac{2E}{m_B} \xi_\perp \left(1 + \frac{\alpha_s C_F}{4\pi} \left[\ln \frac{\mu^2}{m_b^2} + L \right] \right) + \frac{\alpha_s C_F}{4\pi} \Delta V, \\ V_+ &= 0, \\ V_0 &= \frac{E}{m_V} \xi_\parallel \left(1 + \frac{\alpha_s C_F}{4\pi} [-2 + 2L] \right) + \frac{\alpha_s C_F}{4\pi} \Delta V_0, \end{aligned} \quad (47)$$

with $C_F = 4/3$ and $L = -2E/(m_B - 2E) \ln(2E/m_B)$. These expressions hold up to higher-order corrections in α_s , which augment the α_s terms shown, and power corrections.

The α_s -contributions multiplying the soft form factors come from the hard-vertex corrections, and the remaining ones originate from hard scattering with the spectator quark [71],

$$\Delta T_0 = -\frac{m_B^2}{4E^2} \Delta F_\parallel, \quad (48)$$

$$\Delta V_0 = -\frac{q^2}{4E^2} \Delta F_\parallel, \quad (49)$$

$$\Delta V = -\frac{1}{2} \Delta F_\perp, \quad (50)$$

where ΔF_\perp and ΔF_\parallel involve (finite) convolutions of hard-scattering kernels with light-cone distribution amplitudes and can be found in Ref. [71]. Higher-order corrections in α_s do not change the structure or infrared safety of (47), i.e. factorization can be proven to all orders [82]. In particular, the vanishing of T_+ and V_+ at leading power is an all-orders result [20, 83], which looks this simple only

in the helicity basis. The $\mathcal{O}(\alpha_s^2)$ contributions have been calculated in [83–86], and their numerical impact was found to be small, mainly reducing the residual (unphysical) scale dependence.

Thus, in the heavy-quark/large-recoil limit, the form factors T_+ and V_+ exactly vanish. Combining (44) and (47), we have at low q^2

$$T_+(q^2) = \mathcal{O}(q^2/m_B^2) \times \mathcal{O}(\Lambda/m_b), \quad (51)$$

$$V_+(q^2) = \mathcal{O}(\Lambda/m_b). \quad (52)$$

On the other hand, T_0 and V_0 are not suppressed, and are independent of any hadronic information related to the transversal polarizations of the vector meson. Notice also that, with our choice of soft form factors, the vector form factor V , and hence V_- , has a purely residual (higher-order) scale dependence μ at any given order of perturbation theory, from the factorization into the scale-dependent ξ_\perp and a scale-dependent perturbative factor. One can explicitly check that this produces a relative change in the form factor of no more than a 1.5% in the range $m_b/2 \leq \mu \leq 2m_b$.

3.1.2 Numerical values of the $B \rightarrow K^*$ soft form factors

Although the symmetry relations reduce (at leading power) the number of independent non-perturbative functions, for a quantitative treatment one still has to compute the soft form factors by a nonperturbative method and estimate (or calculate) the power corrections. Sum rules formulated on the light cone (LCSR) are customarily used in exclusive B decays to obtain numerical values of the form factors in the large-recoil domain [46, 69, 77]. Other approaches that have been used to calculate the form factors in this regime include local QCD sum rules (QCDSR) [87] and (truncated) Dyson-Schwinger equations (DSE) [88]. We list in Table 1 the results on the $B \rightarrow K^*$ form factors at $q^2 = 0$ and in the transversity basis for the different calculations considered in this paper. The central values of most of the form factors are quite similar, except some (prominently A_0) for which different methods disagree.

A well known issue between the generic results of LCSR calculations (e.g. those of Ref. [77]), QCD factorization, and the SM value of the Wilson coefficient C_7 is that they lead to a branching fraction of the decay $B \rightarrow K^*\gamma$ that is larger than the experimental value. Given that C_7 is constrained to be close to its SM value by the inclusive $B \rightarrow X_s\gamma$ decay rate (at least when assuming $C_7' = 0$ and C_7 real), it is often assumed that this discrepancy is due to a systematic error in the LCSR model which produces an overestimation in the value of the relevant form factor T_1 at $q^2 = 0$ [23]. A possible solution to this problem is to re-scale the form factors such that $T_1(0)$, in combination with the SM value for C_7 , lead to the experimental branching fraction of the radiative decay [39]. Although this procedure discards in part the sensitivity of the $B \rightarrow K^*\ell^+\ell^-$ decay rate to new

Table 1: Values of the $B \rightarrow K^*$ QCD form factors at $q^2 = 0$ in the conventional basis and in the different approaches considered in our study. The uncertainties are those quoted or suggested in the corresponding references (a 15% relative error for the DSE results).

	LCSR [77]	LCSR [46]	QCDSR [87]	DSE [88]
$V(0)$	0.411(33)	0.36^{+23}_{-12}	0.47(3)	0.37(6)
$A_0(0)$	0.374(34)	$0.29^{+0.10}_{-0.07}$	0.30(3)	0.25(4)
$A_1(0)$	0.292(28)	$0.25^{+0.16}_{-0.10}$	0.37(3)	0.28(4)
$A_2(0)$	0.259(27)	$0.23^{+0.19}_{-0.10}$	0.40(3)	0.30(5)
$T_1(0)$	0.333(28)	$0.31^{+0.18}_{-0.10}$	0.38(6)	0.30(5)
$T_3(0)$	0.202(18)	$0.22^{+0.17}_{-0.10}$	0.3	0.27(4)

physics, it does not affect any physical information extracted from asymmetries or ratios, which are, indeed, the most interesting observables in the semileptonic decay [39].

Using the SM value for C_7 and $\mathcal{B}(B \rightarrow K^*\gamma) = (4.33 \pm 0.15) \times 10^{-5}$, one obtains

$$\xi_{\perp}(0) = T_1(0) = 0.277(13), \quad (53)$$

where the error is obtained adding linearly the experimental and the theoretical uncertainties, which come from the SM parameters and the hadronic parameters entering the non-factorizable contributions to the amplitude (shown in Appendix A.2). Re-scaling the values of the form factors in Table 1 and taking the average of the results given by the different models, we obtain

$$\xi_{\parallel}(0) = \frac{2m_{K^*}}{m_B} S(0) = 0.09(2), \quad (54)$$

where we have estimated the uncertainty to be such that it includes the two extreme values coming from the LCSR [77] and DSE [88]. For the q^2 dependence we choose the pole forms introduced in [23] based on pure heavy-quark-limit arguments,

$$\xi_{\perp}(q^2) = \xi_{\perp}(0) \left(\frac{1}{1 - q^2/m_B^2} \right)^2, \quad \xi_{\parallel}(q^2) = \xi_{\parallel}(0) \left(\frac{1}{1 - q^2/m_B^2} \right)^3. \quad (55)$$

In Fig. 1 we plot the form factors T_1 and S in the large-recoil region used in this work as a reference for the symmetry relations in Eqs. (47) with the error bands produced by the uncertainties on $\xi_{\perp}(0)$ and $\xi_{\parallel}(0)$. These are compared with re-scaled central values of the results reported using LCSR [46, 77], QCDSR [87] and DSE [88].

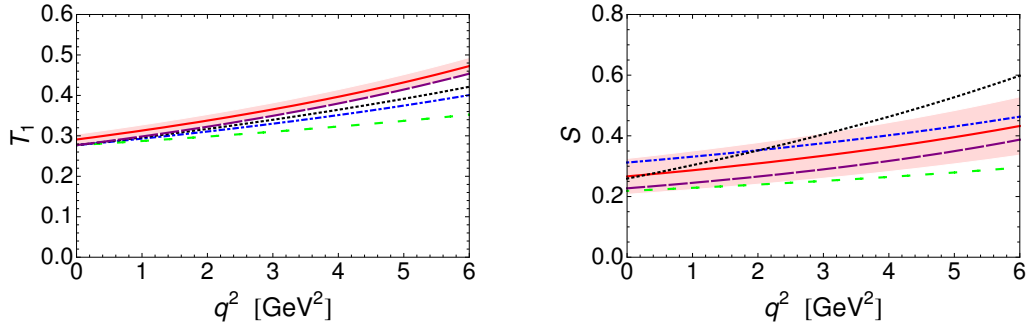


Figure 1: Form factors T_1 and S in the large-recoil region used in this work as a reference for the symmetry relations (thick red line) with the error bands produced by the uncertainties on $\xi_{\perp}(0)$ and $\xi_{\parallel}(0)$. These are compared with the re-scaled (see in the main text) central values of the results obtained in the LCSRs (blue dot-dashed [77] and black dotted [46]), in QCDSRs [87] (green short-dashed) and DSEs [88] (purple long-dashed).

3.1.3 Power corrections to the large-recoil form factor relations

The main factor limiting the utility of QCD factorization for the form factors (and elsewhere) are unknown power corrections $\mathcal{O}(\Lambda/m_b)$. Although one might naively expect such power corrections to be $\sim (5-10)\%$, the possibility of having larger corrections cannot be dismissed. Let us refer to effects breaking the (QCD-corrected) symmetry relations in Eqs. (47) as power corrections, even though these also include the numerically unimportant perturbative α_s^n , $n \geq 2$ contributions. They govern the so-called factorizable power corrections in $B \rightarrow K^* \ell^+ \ell^-$ decay. As they do not cancel out in the “clean” observables defined in [57], estimating them is important to assess hadronic uncertainties. The conventional procedure in phenomenological analyses is to use the results of some technique that automatically includes power corrections (most commonly LCSR). However, in doing so, the systematic errors coming from the assumptions and approximations implied by the particular approach are not transparent. A related issue is that the q^2 -dependence of the form factors is often “hard-coded” and not treated as an uncertainty.

Instead, in this paper we parameterize power corrections to the form factors in a model-independent fashion. The uncertain parameters can then be estimated by various methods. For a given (helicity) form factor F , we parameterize the corrections to (47) as

$$F^{\text{p.c.}} = a_F + b_F \frac{q^2}{m_B^2} + \mathcal{O} \left(\left(\frac{q^2}{m_B^2} \right)^2 ; \Lambda^2/m_b^2 \right), \quad (56)$$

where a_F and b_F are dimensionless numbers of order $\mathcal{O}(\Lambda/m_b)$. Importantly,

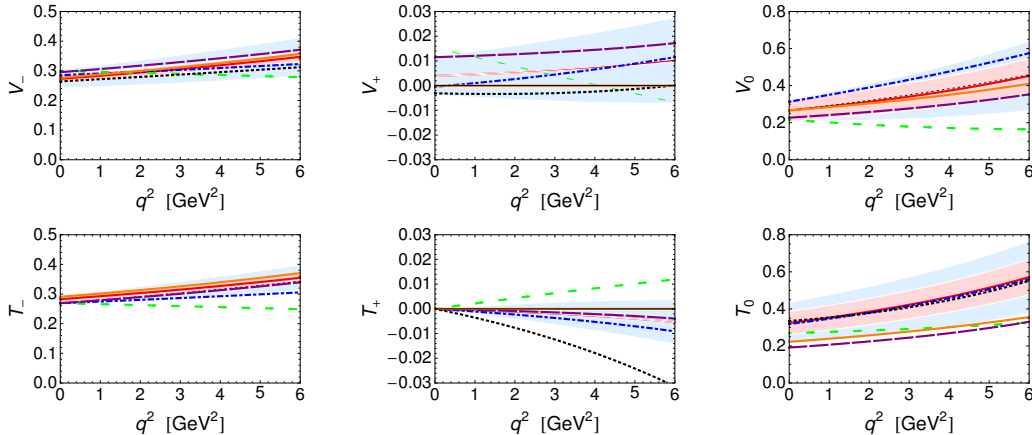


Figure 2: Form factors in the helicity basis and in the large-recoil region used in this work (red thick and solid line). The inner (red) error band is produced by the uncertainties on $\xi_{\perp}(0)$ and $\xi_{\parallel}(0)$, while the outer (blue) includes also the estimated uncertainties on the factorizable power corrections. These curves are compared with the re-scaled central values of the results obtained in the LCSR (blue dot-dashed [77] and black dotted [46] lines), in QCDSR [87] (green short-dashed line) and DSE [88] (purple long-dashed line). For the sake of completeness we also include the curves (orange solid and thin line) obtained in the strict heavy-quark/large recoil limit, Eqs. (47).

Eqs. (44) and (45) imply that $a_{T_+} = 0$ and $a_{V_0} = 0$.

Ideally, the coefficients a_F and b_F should be estimated by a direct calculation of helicity form factors, for example through LCSR (see discussion below). For lack of present availability of such results, we compare available results (in the conventional basis) of the LCSR, QCDSR and DSE approaches to give an estimate of the uncertainty given by the break-down of the symmetry relations. We estimate ranges for the nonvanishing a_F and b_F by taking the average deviations between the results given by the symmetry relations and those obtained in the different models considered in this paper. The resulting ranges are given in Table 2. Note that the a_F are all at the few-percent level, well in line with “naive” expectations about the size of power corrections. The (less important) b_F coefficients are also around the 10-percent level or below, with the exception of the helicity-zero form factors V_0 and, to smaller extent, T_0 . In Fig. 2 we plot our ranges for the form factors, including power corrections described by (56), with the ranges for a_F and b_F given in Table 2. We also show the central values of the results obtained from LCSR [46, 77], QCDSR [87] and in DSE [88],

Our method may over- or underestimate the power corrections. For instance, one would obtain larger uncertainties by combining the LCSR uncertainties on the standard form factors entering V_+ and T_+ in quadrature (or linearly). Hence, our numbers should be considered preliminary until dedicated calculations appear.

Table 2: Bounds on the dimensionless constants a_F and b_F parameterizing the power corrections to the form factor heavy-quark relations.

	V_-	V_+	T_-	T_+	V_0	T_0
$ a _{\max}$	0.027	0.008	0	0	0	0.050
$ b _{\max}$	0.136	0.042	0.125	0.043	0.434	0.206

Nevertheless, it is reassuring that the nonperturbative approaches appear to be consistent with expectations from the heavy-quark limit. In fact, for the LCSR for the form factors the heavy-quark limit has been analyzed a long time ago in [89], and the result is fully consistent with the structure later obtained in [71] and expressed in the helicity basis through (47).

To reduce the LCSR sum-rule uncertainty manifestly, one should derive sum rules directly for the helicity form factors.⁵ To demonstrate this, consider the correlation function

$$G_{F\lambda}(q^2; p^2) = i \int d^4y e^{-ip \cdot y} \langle K^*(k) | T \{ \epsilon_\mu^*(q; \lambda) (\bar{s} \Gamma_F^\mu b) [0] j_B^\dagger(y) \} | 0 \rangle, \quad (57)$$

where $j_B = im_b \bar{q} \gamma_5 b$, q is a light quark field, and Γ_F^μ a Dirac structure appearing in the definition of a given helicity form factor. Its hadronic representation,

$$G_{F\lambda} = \frac{\langle K^*(k, \lambda) | \epsilon_\mu^*(q; \lambda) \bar{s} \Gamma_F^\mu b | B \rangle}{p^2 - m_B^2} \frac{f_B m_B^2}{m_b} + \dots, \quad (58)$$

obtained by inserting a complete set of hadronic states between the two currents, contains the helicity form factor $F_\lambda(q^2) \propto \langle K^*(k) | \epsilon_\mu^*(q; \lambda) \bar{s} \Gamma_F^\mu b | B \rangle$, with the ellipsis denoting contributions from higher resonances and continuum states with the quantum numbers of j_B . A sum rule is obtained from (58) by taking $p^2 < m_B^2$ off-shell by an amount $\mathcal{O}(1 \text{ GeV}^2)$, evaluating $G_{F\lambda}$ perturbatively in a light-cone expansion, and Borel-transforming both sides to suppress the hadronic states above the B . This is completely analogous to the standard sum rules [69], and in fact simpler as the correlation function for a given Γ_F and λ directly gives the respective helicity form factor, with no need for Lorentz decomposition. The light-cone expansion of $G_{F\lambda}$ results in convolutions of perturbative kernels with light-cone distribution amplitudes, which are organised in terms of increasing twist. Let us demonstrate the suppression of the positive-helicity form factors in this framework. At tree level, we have for T_+

$$i \int d^4y e^{-ip \cdot y} T \{ \epsilon_\mu^*(q; +) (\bar{s} \Gamma_T^\mu b) [0] j_B^\dagger(y) \} = \bar{s}(k_1) \epsilon_\mu^*(q; +) q_\nu \sigma^{\mu\nu} P_R \frac{\not{p} - \not{k}_2 + m_b}{(p - k_2)^2 - m_b^2} q(k_2)$$

Now, to leading-twist accuracy we can replace $\bar{s}(k_1)$ and $q(k_2)$ by collinear fields

⁵Such direct calculations have been recently advocated, independently, by T. Feldmann [90].

satisfying $\not{n}_- q = 0$ and $\bar{s} \not{n}_+ = 0$.⁶ As a consequence, we can insert a projector $\bar{s} \rightarrow \bar{s} \frac{\not{n}_- \not{n}_+}{4}$. We then encounter in the Dirac structure a factor

$$\not{n}_- \not{n}_+ \not{\epsilon}^*(q; +) \not{q} P_R$$

It is easy to verify that this vanishes as a consequence of

$$\not{n}_+ \not{\epsilon}^*(q; +) P_L = 0$$

This shows that the correlation function, and thus the form factor T_+ , is suppressed as $\mathcal{O}(\Lambda/E_{K^*}) = \mathcal{O}(\Lambda/m_b)$ as a higher-twist effect. Independently,

$$\not{q} = \frac{n_+ \cdot q}{2} \not{n}_- + \frac{n_- \cdot q}{2} \not{n}_+,$$

where at low $q^2 \ll m_b^2 \sim E_{K^*}^2$ we have $n_+ \cdot q \sim m_b$, while $n_- \cdot q \sim q^2/m_b^2$. Hence up to corrections of $\mathcal{O}(q^2)$, T_+ vanishes as a consequence of

$$\not{\epsilon}^*(q; +) P_L \not{n}_- = 0.$$

In combination, we obtain a behaviour that respects (51). In the analogous case of V_+ , one obtains the behaviour (52) in an analogous way, but no q^2 -suppression (for there is no \not{q} factor in the definition of V_+). For a more quantitative treatment, one needs to go to higher-twist accuracy; this requires going beyond the collinear approximation for the external momenta and quark fields. In principle, the necessary ingredients are known up to twist-4. We leave such an analysis for future work. Note that the argument does not imply a suppression of the helicity-0 form factors.

3.2 Non-Factorizable effects: helicity hierarchies for h_λ

We next turn to the contribution of the hadronic weak hamiltonian in rare semileptonic B -decays. As explained above, these contributions enter only in $H_V(\lambda)$, via h_λ defined through (11) and (23). They do not naively factorize into form factors and leptonic currents, but involve the B to V matrix elements of a T -product of the weak hamiltonian and an electromagnetic current $\langle V | T(j^{\text{em, had}, \mu}(y) \mathcal{H}_{\text{eff}}^{\text{had}}(0)) | \bar{B} \rangle$. A systematic treatment based on QCD factorization exists [23, 29], to leading power in an expansion in Λ/m_b . Contributions can be divided into “form factor correction”, “annihilation”, and “spectator-scattering” terms and are given in terms of (soft) form factors, hard-scattering kernels, and light-cone distribution amplitudes, as in the form factor relations discussed above. Power corrections do not, in general, factorize. Only a subset

⁶We are assuming the K^* to move in the $+\hat{z}$ direction here, as throughout the present paper. Note that in the relevant literature on LCSR for form factors, the final-state hadron is often taken to be moving in $-\hat{z}$ direction instead.

of Λ/m_b power corrections to $B \rightarrow V\ell^+\ell^-$ have been studied in the literature, in the context of isospin asymmetries [27, 28]. Some of these contributions violate factorization and were modelled in a standard way [27, 91].

Importantly, QCD factorization predicts that the suppression of the positive-helicity amplitudes continues to hold in the presence of non-factorizable terms [23], and it is also true for the known power corrections [27, 28]. That is, h_+ still vanishes at this order, and this is again a direct consequence of the $V-A$ structure of SM weak interactions. For h_- , the known power corrections do not vanish, and result in an isospin asymmetry of about 10% at $q^2 = 0$, rapidly falling with increasing q^2 . For the isospin-averaged branching fraction, this reduces to about a 3% effect [from a replacement $e_u - e_d \rightarrow e_u + e_d$]. However, the modelling of (incalculable) power corrections is not necessarily accurate, and it is in particular important to investigate to what extent h_+ may be generated by them.

In the following, we separate the hadronic weak hamiltonian into a charm part (with large CKM and Wilson coefficients), a gluonic part (Q_{8g} , with a large CKM and Wilson coefficient), and a light-quark part (involving only operators which are suppressed by small CKM elements or by small Wilson coefficients), and investigate in each case the possible sizes of power corrections, in particular to h_+ , by methods complementary to QCDF.

3.2.1 Charm loop

Within the context of LCSR, a study of charm loop effects at low q^2 has been given recently by Khodjamirian et al [46], and the analogous contributions to $B \rightarrow K^*\gamma$ have been considered earlier in [34]. In [46], long-distance charm-loop effects are estimated to be sizable (and with large uncertainties); these effects correspond in part to power corrections in QCDF. Unfortunately, the results in [46] are only presented in a numerical form and only for transversity, not helicity, amplitudes, expressed through effective (amplitude-dependent) shifts of the Wilson coefficients C_9 . Nevertheless, central values and uncertainties given there are suggestive of a strong correlation of the charm loop contributions to A_{\parallel} and A_{\perp} and a suppression $h_+ \ll h_-$. The computation in [34] provides directly results for h_+ and h_- at $q^2 = 0$, both of them numerically smaller, implying also h_- much smaller than suggested by [46].

The aim of this section is to argue that a hierarchy $h_+ \ll h_-, h_0$ results, as far as the charm loop goes, from the light-cone dominance of the amplitude at $q^2 \ll m_B^2$. To this end, let us recast the strategy of [46] in terms of helicity amplitudes, picking out the charm loop in h_{λ} ,

$$h_{\lambda}|_{c\bar{c}} = \frac{1}{m_B^2} \frac{2}{3} \epsilon_{\mu}^*(\lambda) \int d^4y e^{iq \cdot y} \langle M|T\{(\bar{c}\gamma^{\mu}c)(y)(C_1^c Q_1^c + C_2^c Q_2^c)(0)\}|\bar{B}\rangle. \quad (59)$$

Next, [46] shows that the Fourier integral is dominated by the light-cone $y^2 \approx 0$. A light-cone OPE is then performed. To leading order, this results in a local op-

erator whose matrix elements can be identified with the charm-loop contribution to the form factor term in QCDF (ie those charm-loop effects that do not involve the spectator quark). At the one-gluon level, one has the expression

$$h_\lambda|_{c\bar{c},\text{LD}} = \epsilon^{\mu*}(\lambda)\langle M(k, \lambda)|\tilde{\mathcal{O}}_\mu|\bar{B}\rangle, \quad (60)$$

where

$$\tilde{\mathcal{O}}_\mu = \int d\omega I_{\mu\rho\alpha\beta}(q, \omega)\bar{s}_L\gamma^\rho\delta\left(\omega - \frac{in_+\cdot D}{2}\right)\tilde{G}^{\alpha\beta}b_L, \quad (61)$$

with D the covariant derivative and $I_{\mu\rho\alpha\beta}$ given in [46]. The nonlocal operator (61) is the first subleading term in an expansion in $\Lambda^2/(4m_c^2 - q^2)$, with terms involving two and more gluon fields contributing only at higher orders [46]. Eq. (60) hence provides an approximation to the long-distance charm-loop contributions. It *can* be further expanded in local operators,

$$\tilde{\mathcal{O}}_\mu^{(n)} = \frac{1}{n!}\frac{d^n}{d\omega^n}I_{\mu\rho\alpha\beta}(q, \omega)\Big|_{\omega=0}\bar{s}_L\gamma^\rho\left(\frac{in_+\cdot D}{2}\right)^n\tilde{G}^{\alpha\beta}b_L. \quad (62)$$

The result of [34] corresponds to keeping only the $n = 0$ term, and evaluating its matrix element by means of a LCSR for a correlation function

$$i\int d^4y e^{-ip\cdot y}\langle K^*|[\tilde{\mathcal{O}}_\mu^{(0)}(q)](0)j_B^\dagger(y)|0\rangle. \quad (63)$$

Ref. [34] argued the suppression of higher terms in the local OPE by a *larger* expansion parameter of order $m_B\Lambda/(4m_c^2)$, which has been taken as (20 – 40)% and used to justify truncating the OPE after the leading term. This numerical value corresponds to taking $\Lambda \sim 300\text{--}650$ GeV (for $\overline{\text{MS}}$ quark masses), and should hold up to an $\mathcal{O}(1)$ factor, which if large could in principle spoil the convergence of the OPE. More seriously, the power counting itself was obtained by appealing to inclusive $B \rightarrow X_s\gamma$ decay, where similar matrix elements $\langle B|\bar{b}(q\cdot D)^n G_{\alpha\beta}\Gamma b|B\rangle$ occur as part of power corrections to the charm loop [92, 93]. (Γ denotes a Dirac structure which is irrelevant to the present discussion.) There, the softness of the B meson constituents provides one power of Λ in the numerator, which can be seen via $q\cdot D \supset -iq\cdot k_G \sim m_b\Lambda$, where k_G is the gluon momentum [92]. (The resulting ‘suppression’ factor is estimated as 0.6 in [93].) However, with an energetic K^* in the final state as in (63) the constituents have energies $\mathcal{O}(m_b)$, so $n_+\cdot D \supset n_+\cdot k_G \sim m_b$ and a scaling $m_b^2/(4m_c^2)$ of the putative expansion parameter seems appropriate; at least, establishing a suppression requires a new argument. We therefore will not rely on the estimate of [34] in this paper. Ref. [46] estimates instead the full nonlocal operator matrix element from a LCSR for a different correlation function

$$\langle 0|T\{j_\nu^{K^*}(y)\tilde{\mathcal{O}}_\mu(0)\}|B\rangle, \quad (64)$$

where $j_\nu^{K^*} = \bar{d}\gamma_\nu s$, which yields the matrix element in terms of B -meson LCDAs.

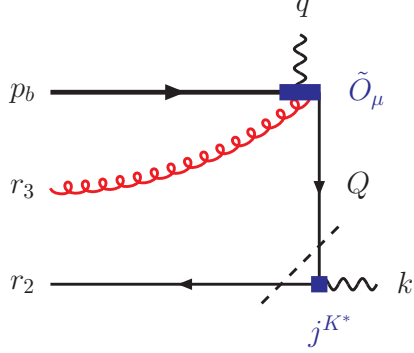


Figure 3: Tree-level diagram for the light-cone OPE for the correlation function (65). The dashed line indicates a two-particle cut contributing to the (perturbative) spectral density.

To show the suppression of h_+ , note that h_{\pm} can be obtained directly from

$$G_{h\lambda}(q^2; k^2) = -i \int d^4y e^{iky} \langle 0 | T \{ \epsilon^{\nu*}(\hat{z}; \lambda) j_{\nu}^{K^*}(y) \epsilon^{\mu*}(-\hat{z}; \lambda) \tilde{O}_{\mu}(0) \} | B \rangle. \quad (65)$$

To be precise, we take $k = (k^0, 0, 0, |\mathbf{k}|)$, as well as q , in the (tz) plane. Note that for $\lambda = \pm$ the polarisation 4-vectors are (with these conventions) independent of \mathbf{k} , hence the rhs indeed defines a Lorentz-invariant function of k^2 and q^2 . (The formalism could, with appropriate care, be extended to $\lambda = 0$.) The hadronic representation contains the desired matrix element,

$$G_{h\lambda}(q^2; k^2) = \frac{f_{K^*} m_{K^*}}{m_{K^*}^2 - k^2} \langle K^*(\tilde{k}; \lambda) | \epsilon^{\mu*}(-\hat{z}; \lambda) \tilde{O}_{\mu}(0) | B \rangle + \text{continuum contributions}. \quad (66)$$

Here $\tilde{k} = (\sqrt{m_{K^*}^2 + \mathbf{k}^2}, 0, 0, |\mathbf{k}|)$ is the physical (on-shell) 4-momentum of the K^* corresponding to the given q^2 . To obtain a LCSR, following [46] we take $k^2 \sim -1\text{GeV}^2 \sim -m_b\Lambda$ (corresponding to a Borel parameter $\sim \sqrt{m_b\Lambda}$) and consider the light-cone OPE of $G_{h\lambda}$. The leading (tree) diagram is shown in Fig. 3. Defining $n_+ \cdot q \equiv m_B + l$, and taking the b -quark momentum to be $p_b = m_b/2(n_+ + n_-) + r_1$, we have $l \sim \Lambda > 0$ and

$$q = m_b \frac{n_-}{2} + \frac{q^2}{m_b + l} \frac{n_+}{2}, \quad (67)$$

$$k = m_b \frac{n_+}{2} + \mathcal{O}(\Lambda), \quad (68)$$

$$Q = m_b \frac{n_+}{2} + \mathcal{O}(\Lambda), \quad (69)$$

such that $Q^2 \sim m_b\Lambda$, making the internal propagator, in QCDF/SCET terminology, a hard-collinear line. The operator product, to tree level, becomes

$$\epsilon_{\nu}^*(\hat{z}, \lambda) \gamma^{\nu}(k) \frac{Q + m_s}{Q^2 - m_s^2} P_R \epsilon^{\mu*}(-\hat{z}; \lambda) \tilde{O}_{\mu}(q), \quad (70)$$

where P_R has been inserted for convenience [note that $\tilde{O}_\mu(q)$ contains a chiral projector]. Neglecting terms $\mathcal{O}(\Lambda, m_s)$ in the propagator, this vanishes for $\lambda = +$. Hence the nonlocal charm loop contribution to h_+ is $\mathcal{O}(\Lambda/m_b)$ -suppressed relative to h_- , and altogether

$$h_+|_{c\bar{c},\text{LD}} = \mathcal{O}\left(\frac{\Lambda^3}{4m_c^2 m_b}\right) \quad (71)$$

relative to the leading-power amplitude H_V^- . Nevertheless, we will see below that it constitutes the dominant remaining source of theoretical uncertainty on several “clean” observables, thanks to the strong suppression of the helicity form factor T_+ . This shows at the same time the importance of taking it into account, and motivates further, more quantitative work on the nonlocal power-corrections to (mainly) the positive-helicity amplitudes.

Unlike in the form factor case, the more traditional LCSR of Ref. [34], involving the correlation function (63) with an on-shell K^* rather than a B , does not lend itself to an analogous argument. Essentially, the reason is that that sum rule is given in terms of (most importantly) chiral-even twist-3 3-particle LCDAs, where, loosely speaking, the helicity of the meson is determined by that of the gluon field-strength tensor, whereas the helicities of the quark and anti-quark fields cancel out. Hence the presence of a chiral projector has no direct impact on the helicity of the K^* . Of course the suppression should still be seen in the numerical result for the full (rather than lowest-order local OPE) result. However, higher-order terms in the local OPE are not known, nor do they seem to be suppressed, as argued above.

3.2.2 Chromomagnetic penguin operator

The operator Q_{8g} comes with a large CKM factor and its Wilson coefficient is not small. In QCDF, it enters exclusively through the hard spectator scattering contributions. These factorize at leading power, but at order Λ/m_b , attempting to factorize them results in endpoint divergences [27], implying a breakdown of factorization. Cutting off the end point divergence and modelling the end-point contribution as in [27, 28], h_+ still vanishes at subleading power. However, on general grounds one would expect chirality-violating QCD (and strange mass) effects to generate a contribution to h_+ at order Λ/m_b and m_s/m_b . It is possible to estimate the Q_{8g} contribution to h_λ with a LCSR, similarly to the sum rule for the nonlocal operator \tilde{O}_μ . For $B \rightarrow K\ell^+\ell^-$ (where the dilepton helicity $\lambda = 0$), such a calculation has been very recently performed in [94], wherein a “soft” contribution is identified and expressed in terms of three-particle B -meson light-cone distribution amplitudes. The operator \tilde{O}_μ is replaced by the simpler (local) Q_{8g} , but the required correlation function involves an extra insertion of the electromagnetic current anywhere on the quark line in Fig. 3.

Here, we note that our above argument showing a helicity hierarchy of the long-distance charm loop contributions likewise can be applied to this sum rule

for the matrix element of Q_{8g} . The operator Q_{8g} still provides a chiral projector, and the fermion line entering j^{K^*} in Fig. 3 is still “hard-collinear”, such that the first four factors in (70) are unchanged, even if the electromagnetic current insertion occurs on that line (if the strange quark mass is neglected). The result is again that the long-distance (soft) contribution $h_+|_{Q_{8g},\text{LD}}$ is suppressed by Λ/m_b or m_s/m_b relative to $h_-|_{Q_{8g},\text{LD}}$. As the latter is already suppressed by a power of Λ/m_b relative to the leading-power amplitude H_V^- , the impact on Q_{8g} on h_+ should be negligible. (Note also that the effect of the “soft” Q_{8g} contributions in $B \rightarrow K\ell^+\ell^-$ was found to be well below 1 % of the total hadronic contribution in [94]. It is difficult to see how a much larger contribution could occur in the present case, even for the non-helicity-suppressed amplitude h_- .)

3.2.3 Light quarks and resonance structure

The remaining contributions of the hadronic weak Hamiltonian to the decay amplitude coming from the QCD penguin operators and the double Cabibbo-suppressed current-current operators involving up quarks,

$$a_\mu^{\text{had,lq}} = \int d^4x e^{-iq\cdot x} \langle \bar{K}^* | T \{ j_\mu^{\text{em}}(x), \mathcal{H}_{\text{eff}}^{\text{had,lq}}(0) \} | \bar{B} \rangle, \quad (72)$$

and are either doubly Cabibbo-suppressed or weighted by the small Wilson coefficients C_{3-6} . Again, a systematic description exists within QCDF [23], with a vanishing contribution to h_+ at leading power and a breakdown of factorization at subleading powers. Because of the multiple suppression factors, the contributions to H_V^+ arising in this fashion are negligible.

However, long-distance non-perturbative effects may manifest themselves partly as resonances or poles in the complex- q^2 plane, implying a resonance structure which we do not expect to be accounted for at any order in Λ/m_b . Therefore we employ a hadronic description to estimate both power corrections and the possibility of large “duality-violating” effects in $B \rightarrow K^*\ell^+\ell^-$ observables. In order to do this, let us consider instead the object

$$\tilde{a}_\mu^{\text{had,lq}} = \int d^4x e^{-iq\cdot x} \langle \bar{K}^* | T \{ j_\mu^{\text{em,lq}}(x), \mathcal{H}_{\text{eff}}^{\text{had}}(0) \} | \bar{B} \rangle, \quad (73)$$

where we only keep the light-quark part of the electromagnetic current, relevant for resonance structure in the low- q^2 region (but revert to the full weak Hamiltonian). Ideally, we would like to compute $\tilde{a}_\mu^{\text{had,lq}}$ taking into account the fact that pions and other light hadrons are the relevant degrees of freedom of QCD in this domain, in a systematic fashion as, for example, using chiral perturbation theory (χ PT) [95, 96], together with any of the methods that extend its range of applicability up to the region of the light resonances [97–100]. In fact, this program is attainable for kaon decays in which the energies and masses are all small compared with the chiral symmetry breaking scale $\Lambda_{\chi SB} \sim 1 \text{ GeV}$ [101]. In

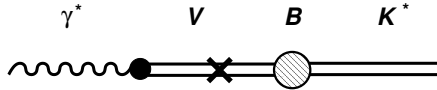


Figure 4: Graphical representation of the VMD model. The filled bulb represents the $\bar{B} \rightarrow V \bar{K}^*$ decay vertex, as obtained in QCD factorization, the solid bulb f_V , as obtained from experiment, and the double lines resonance propagators, with the cross indicating the multi-particle dressing of the respective pole.

case of the B -meson decays, one encounters heavier scales and, at present, it is not clear how to integrate them out in order to extract the long-distance effects in a model-independent way [102, 103].

In this paper we use a model to estimate the contribution of the light hadronic degrees of freedom in the low- q^2 region. We start by making a factorization approximation of the correlation function Eq. (73), using a basis of hadronic states $|P(0)\rangle$ and $|P'(x)\rangle$,

$$\tilde{a}_\mu^{\text{had, lq}} = \int d^4x e^{-iq \cdot x} \sum_{P, P'} \langle 0 | j_\mu^{\text{em, lq}}(x) | P' \rangle \langle P'(x) | P(0) \rangle \langle \bar{K}^* P | \mathcal{H}_{\text{eff}}^{\text{had}}(0) | \bar{B} \rangle, \quad (74)$$

where the sums include further integrations for multi-particle states. We next assume that these sums are saturated by the lightest neutral vector resonances $V = \rho(770)$, $\omega(782)$ and $\phi(1020)$, i.e. vector meson dominance (VMD). This hypothesis has proven very fruitful in modelling the electromagnetic structure of light hadrons at low energies. It finds microscopic justification in the large N_c limit of QCD [104] and it has been successfully implemented to connect the short-range part of the low-energy interactions of pions with QCD [97, 98]. (For a compilation of phenomenological applications of the model in the weak decays of mesons see Ref. [105].) In the VMD, the first factor in the RHS of Eq. (74) is a semileptonic decay constant, f_V , the second the vector-meson propagator and the third a $\bar{B} \rightarrow V \bar{K}^*$ decay amplitude. Finally, we (partially) take into account the effect of the continuum of multi-particle hadronic states by dressing the poles of the resonance by their (off-shell) width. All in all, the estimate for the hadronic contribution at low q^2 can be pictured as in Fig. 4.

In order to carry out the computation, it is convenient to use an effective Lagrangian containing fields which serve as interpolators for the vector resonances. We choose the anti-symmetric representation advocated in Refs. [97, 98] for applications in χ PT. Other Lagrangian formulations consistent with chiral symmetry and electromagnetic gauge invariance⁷ are equivalent to this one, once consistency

⁷Notice that in a previous VMD analysis [106] of the vector-meson contribution to the $B \rightarrow K^* \ell^+ \ell^-$ decay, electromagnetic gauge and non-gauge invariant Lagrangians were considered in the same footing and large differences between the two approaches have been reported at low q^2 . In this paper we work exclusively with approaches consistent with electromagnetic gauge symmetry (and QCD, as stated in the main text).

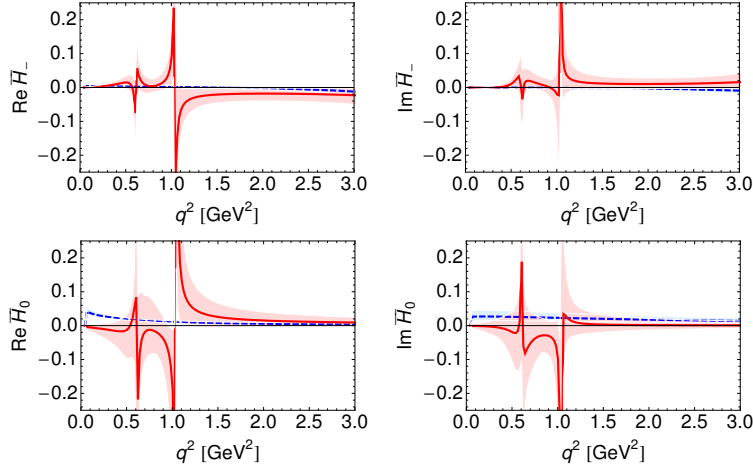


Figure 5: Relative contribution (see main text) of the light-quark component of the electromagnetic current to the helicity amplitudes H_-^V and H_0^V . The dashed (blue) line is the result in QCD factorization while the solid (red) line is the result in the hadronic model used in this work.

with QCD asymptotic behavior of 2-point spectral functions is demanded [98]. We address the reader to Appendix B for the details and conventions used in the model.

As for the $\bar{B} \rightarrow V\bar{K}^*$ decay amplitude, it is natural, in the present context, to use the QCD factorization calculation reported in Ref. [107]. In fact, as already discussed in [23], there is a one-to-one correspondence between a subclass of diagrams in the QCDF calculation of $\bar{B} \rightarrow \bar{K}^*\ell^+\ell^-$ and of the diagrams appearing in the QCDF calculation for $\bar{B} \rightarrow V\bar{K}^*$, where V is one of the light-quark resonances. For our model calculation, we employ the QCDF results for the $B \rightarrow V\bar{K}^*$ amplitudes, while at the same time omitting the corresponding terms from the $\bar{B} \rightarrow \bar{K}^*\ell^+\ell^-$ amplitude. Next, the heavy-quark limit predicts a hierarchy of helicity amplitudes, $H_0 : H_- : H_+ = 1 : \Lambda/m_b : \Lambda^2/m_b^2$, i.e. in relative terms $H_+/H_- \sim \Lambda/m_b$. Although H_- and H_+ do not factorize in QCDF, as the hard-scattering contributions develop end-point singularities, and the hierarchy $H_0 \gg H_-$ is numerically removed by large penguin corrections (obviating the so-called polarization puzzle [108]), the hierarchy $H_+ \ll H_-, H_0$ remains and is in good agreement with experiment in $\bar{B}^0 \rightarrow \bar{K}^{0*}\phi$ decays, for which complete angular analyses exist [109, 110]. An important consequence of this is that both in QCDF and in our model, the contribution to the $\bar{B} \rightarrow \bar{K}^*\ell^+\ell^-$ “wrong-helicity” amplitude is suppressed as

$$h_+^{\text{had, lq}}/h_0^{\text{had, lq}} = \mathcal{O}(\Lambda/m_b)^2, \quad h_+^{\text{had, lq}}/h_-^{\text{had, lq}} = \mathcal{O}(\Lambda/m_b), \quad (75)$$

on top of the smallness already implied by the CKM factor and Wilson coefficients. As a result, we expect the light-quark hadronic pollution of observables

sensitive to the chirality-flipped operator Q_7' to be negligible, and preclude in particular large “duality-violating” corrections to the leading-power QCDF results for $\bar{B} \rightarrow \bar{K}^* \ell^+ \ell^-$. Thus, in the phenomenological section we set $h_+^{\text{had, lq}} = 0$.

In Fig. 5 we compare the model calculation to that obtained from the corresponding subclass of QCDF diagrams. More precisely, in order to show their relative impact on the helicity amplitudes, we plot $\bar{H}_- = H_-^{\text{lq}}/H_-^V$ and $\bar{H}_0 = H_0^{\text{lq}}/H_0^V$. The two approaches agree on the relative smallness of these terms, of a few percent, across most part of the low q^2 region. Remarkably, this continues to be true in the upper part, despite the fact we are neglecting the excited vector mesons ρ^* , ω^* and ϕ^* that populate the region $q^2 \gtrsim 2 \text{ GeV}^2$. In this regard, we point out that these states have a sub-dominant effect in the hadronic structure of the electromagnetic current as it is, indeed, probed in e^+e^- annihilation experiments. Therefore, one would expect their contribution to produce some oscillations in the hadronic determination converging, approximately, to the QCDF result at larger q^2 . In the numeric computations we ignore these higher-mass resonance contributions and we enforce a continuous matching onto the QCDF result at the threshold $q^2 \sim 2 \text{ GeV}^2$ by means of a suitable q^2 -dependent smearing function (see Appendix B).

On the other hand, in the regions around the resonance poles, the discrepancy between the two approaches is maximal and the hadronic model gives contributions which are comparable in magnitude to the leading ones. In order to discuss this in more detail, consider the schematic form of the semileptonic decay amplitude (see Appendix B),

$$\mathcal{M}_T = \mathcal{M} + \epsilon \frac{8\pi Q_V f_{K^*} f_V}{(q^2 - m_V^2 + im_V \Gamma_V)} \mathcal{M}',$$

given by the interference of the leading piece \mathcal{M} including the effects of the electromagnetic and semileptonic penguin coefficients $C_{7,9,10}$ and \mathcal{M}' , the $\bar{B} \rightarrow V \bar{K}^*$ amplitude normalized such that $|\mathcal{M}| \sim |\mathcal{M}'|$ and $\epsilon \sim \lambda_{\text{CKM}}^2 \sim 0.05$. Then,

$$\begin{aligned} |\mathcal{M}_T|^2 &= |\mathcal{M}|^2 + \epsilon^2 \frac{(8\pi Q_V f_{K^*} f_V)^2}{(q^2 - m_V^2)^2 + m_V^2 \Gamma_V^2} |\mathcal{M}'|^2 \\ &+ 2\epsilon \frac{8\pi Q_V f_{K^*} f_V}{(q^2 - m_V^2)^2 + m_V^2 \Gamma_V^2} \left\{ (q^2 - m_V^2) \text{Re}[\mathcal{M}^* \mathcal{M}'] + m_V \Gamma_V \text{Im}[\mathcal{M}^* \mathcal{M}'] \right\}. \end{aligned}$$

The contribution of the resonances to the decay rate is sizable and potentially of the same order as the leading one only within a q^2 -region of width $\sim m_V \Gamma_V$ around the position of their poles, in which $\epsilon \times (f_V f_{K^*} / m_V \Gamma_V) \sim 1$. This means, at the same time, that integrating over a large enough region of q^2 , $\Delta q^2 \gg m_V \Gamma_V$, suppresses their relative contributions by a factor $m_V \Gamma_V / \Delta q^2$. Therefore, we conclude that although the effects of the light resonances could alter the line shape of observables, they are largely washed out by binning in q^2 . We will see this explicitly in the results presented in the next section.

3.3 Summary and phenomenological implementation

In the preceding two subsections we have studied hadronic effects in the contributions of the various parts of the weak $\Delta B = 1$ effective hamiltonian to the helicity amplitudes. Our main outcome is a strong suppression of the helicity amplitudes H_V^+ and H_A^+ , which in turn suppresses the coefficients I_3 and I_9 in the angular distribution.

- At the factorizable level, this comes about through a double suppression of T_+ by q^2/m_B^2 and Λ/m_b , and a single suppression of V_+ by Λ/m_b . In the absence of right-handed currents (primed Wilson coefficients) this translates to suppressed H_V^+ and H_A^+ .
- The contributions of the hadronic weak Hamiltonian enter only into H_V^+ , via h_+ defined in (23). They are calculable at the leading power in an expansion in Λ/m_b in QCDF. At this order, $h_+ = 0$.
- Long-distance “charm loop” effects can be studied in an expansion $\Lambda^2/(4m_c^2 - q^2)$. At zeroth order, one recovers the non-factorizable form factor QCDF expressions, which give vanishing contributions to h_+ . The first nonzero, long-distance, contribution to h_+ arises at order $\Lambda^3/(4m_b m_c^2)$ relative to the amplitudes H_V^- and H_V^0 . Long-distance contributions of the chromomagnetic operator Q_{8g} are expected to be small, with the contribution to h_+ suppressed (at least) as Λ^2/m_b^2 .
- The remaining effects are suppressed by small CKM and Wilson coefficients. We estimate long-distance corrections to QCDF by means of a resonance (VMD) model, which embodies a suppression of the contribution to h_+ , as a consequence of the helicity structure in $\bar{B} \rightarrow V \bar{K}^*$ decay. After binning the model predicts very small corrections in the other amplitudes h_- and h_0 .

In our phenomenological analysis, we employ our model-independent parameterisation of form factors through (55) and (56) (keeping terms up to and including $\mathcal{O}(q^2/m_B^2)$), together with the numerical values and ranges given in Sect. 3.1. For the contributions of the hadronic weak Hamiltonian, we employ the leading-power QCD factorization expressions [23, 29]. To estimate the long-distance corrections, we employ the following model for long-distance charm loop effects,

$$h_-|_{c\bar{c},\text{LD}} = 0.1 e^{i\phi_-} C_7^{\text{SM}}, \quad (76)$$

$$h_+|_{c\bar{c},\text{LD}} = 0.02 e^{i\phi_+} C_7^{\text{SM}}, \quad (77)$$

where ϕ_{\pm} are arbitrary soft rescattering phases, comprising a conservative interpretation of the numerical findings of [46] and the hierarchy $h_+ \ll h_-$. We will also allow for an extra long-distance contribution $h_0|_{c\bar{c},\text{LD}} = 0.2 e^{i\phi_0} C_7^{\text{SM}}$, as there

is no power suppression of h_0 ; this should be considered an ad hoc model but does not impact on the observables emerging as clean in the phenomenological analysis below, which only involve helicities ± 1 . We have increased the magnitude of these effects beyond the error estimates of [46], such as to accommodate within it the small long-distance contributions from the chromomagnetic penguin operators. For the light-quark Hamiltonian, we estimate possible long-distance corrections by means of the model described in Sect. 3.2.3. Input parameters are summarized in Appendix A.2.

4 Phenomenology at low q^2

4.1 Observables for $\bar{B} \rightarrow \bar{K}^* \ell^+ \ell^-$

In general, there are twelve q^2 -dependent observables (shown in [39] neglecting tensor operators, but this remains true in their presence) that are accessible through a full-angular analysis of the $\bar{B} \rightarrow \bar{K}^* \ell^+ \ell^-$ decay rate and which correspond to the angular coefficients $I_i(q^2)$ in Eq. (38). In the absence of scalar and tensor operators, which includes the SM, $I_6^c = 0$, and there is one relationship among the remaining coefficients, reducing the number of independent observables to ten [45]. If one furthermore assumes $m_\ell = 0$, two more relations can be established,

$$3I_{1s} = I_{2s}, \quad I_{1c} = -I_{2c}, \quad (78)$$

leading to eight independent observables.

The analysis of the CP-partner decay $B \rightarrow K^* \ell^+ \ell^-$ gives a same amount of independent observables as in the \bar{B} decay, the \bar{I}_i 's. In this sense, it is useful to define the following combinations of I_i 's and \bar{I}_i 's,

$$\Sigma_i = \frac{I_i + \bar{I}_i}{2}, \quad \Delta_i = \frac{I_i - \bar{I}_i}{2}, \quad (79)$$

which can be used to construct a variety of CP-averages and asymmetries [37, 39].

4.2 The $\bar{B}^0 \rightarrow \bar{K}^{*0} \mu^+ \mu^-$ decay

In Fig. 6, we show the SM predictions for the eleven angular coefficients available in this case and normalized by the \bar{B}^0 decay rate at low q^2 . The solid (red) and the dashed (green) lines correspond to the prediction including the light-quark contributions in the hadronic model or in QCD factorization, respectively (see Sec. 3). The inner (red) error band is the uncertainty derived from the hadronic parameters (soft form factors, decay constants, . . .), the CKM parameters and the renormalization scale. The intermediate (blue) and outer (green) bands result from the addition in quadratures of the unknown factorizable and charm-loop

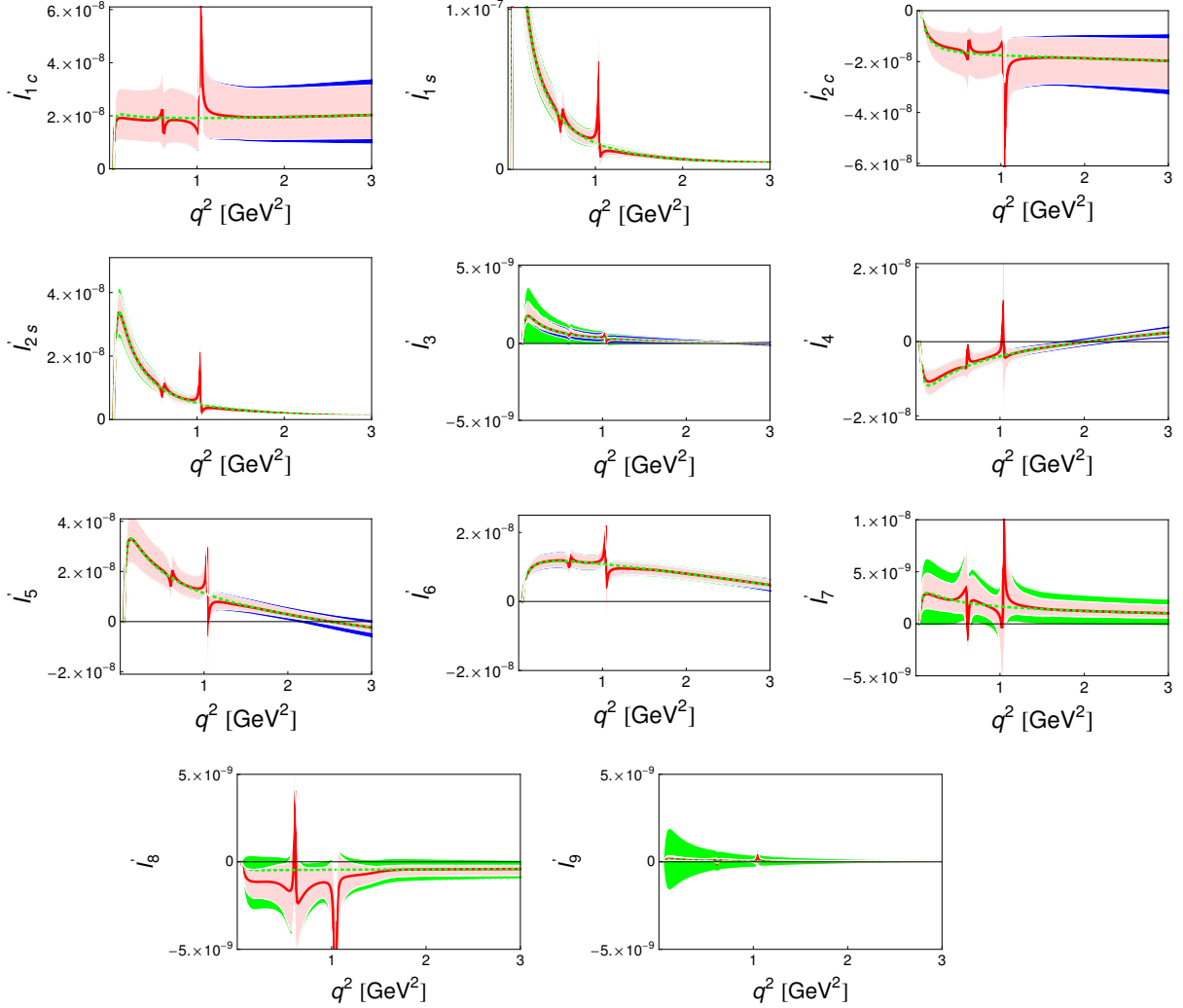


Figure 6: Angular coefficients normalized by the \bar{B}^0 decay rate (I'_i) around the low- q^2 end-point. Solid (red) and dashed (green) lines correspond to the SM prediction including the light-quark contributions in the hadronic model or QCD factorization, respectively. The error bands stem from the hadronic and CKM uncertainties and renormalization scale dependence (inner-red), plus the unknown factorizable power-corrections (internal-blue) and plus the non-factorizable charm-loop uncertainty (outer-green). The errors are added, subsequently, in quadratures.

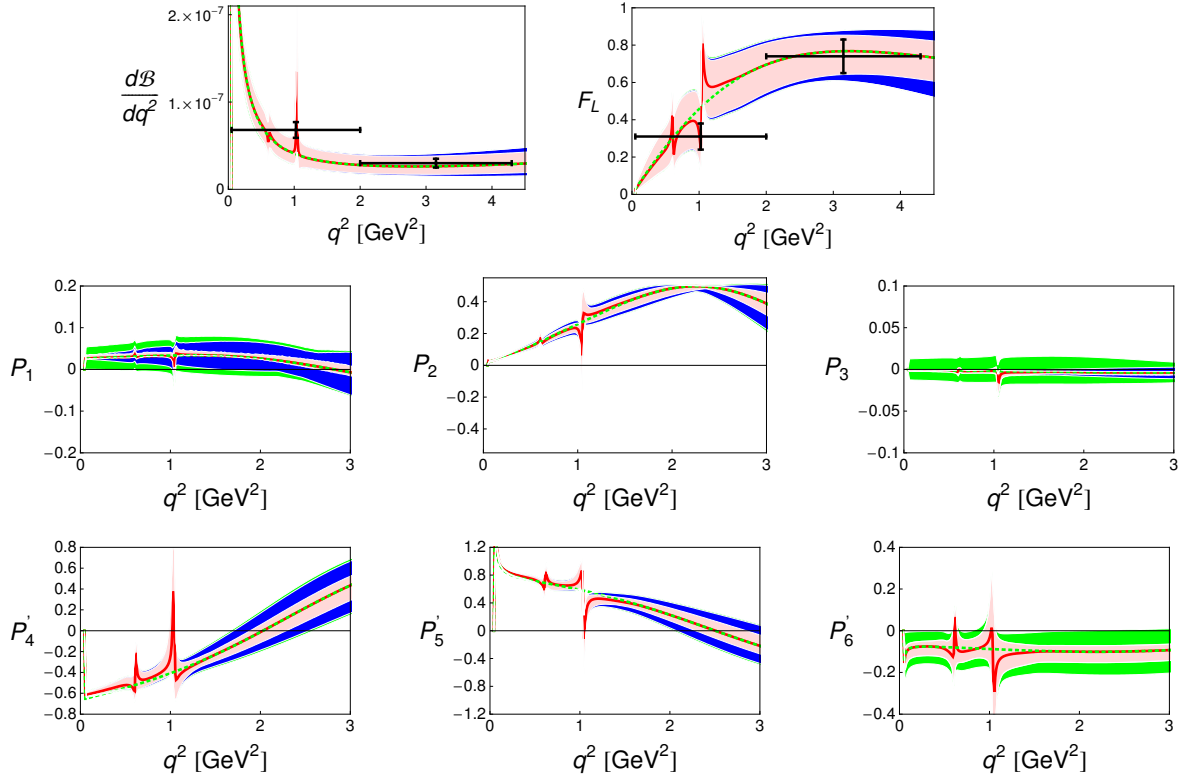


Figure 7: Differential branching fraction, F_L and the “clean” observables $P_i^{(\prime)}$ around the low- q^2 end-point. We show in black the experimental results for the two first observables in the bins $[0.05, 2]$ GeV² and $[2, 4.3]$ GeV² [6]. The color code is as in Fig. 6.

power corrections, subsequently. Factorizable corrections are estimated using Eq. (56), and the charm-loop uncertainty are modelled according to Eqs. (77).

The main source of uncertainties in the I_i 's stem from the soft form factors and, in some cases, from the charm-loop. In particular, for the coefficients proportional to $H_{V,A}^+$, I_3 and I_9 , the latter source is, by far, the most important. On the other hand, it is remarkable that the uncertainties in the coefficients arising from the unknown factorizable power corrections are negligible at low q^2 . This effect is due to the constraints imposed by the exact relations (44). Finally, notice that the vector-meson resonances alter significantly the line shape of most of the I_i 's, except for those $\propto H_{V,A}^+$ due to the suppression of the corresponding helicity amplitude in the $\bar{B} \rightarrow \bar{K}^*V$ decays (see Sec. 3).

4.2.1 CP-averages: The branching fraction, F_L and the P -basis

Each of the observables that can be constructed out of the CP combinations in Eqs. (79) has a different sensitivity to the various standard and non-standard Wilson coefficients. In order to maximize these sensitivities, it is important to find a set of observables with reduced dependence to the uncertain hadronic parameters underpinning the theoretical predictions, in particular the $B \rightarrow K^*$ form factors [32, 38]. Indeed, a proper set of “clean” observables can be obtained using suitable ratios of angular coefficients [53, 57, 66]. Following this strategy, we use the following set of CP-averaged observables [66],

$$P_1 = \frac{\Sigma_3}{2\Sigma_{2s}}, \quad P_2 = \frac{\Sigma_6}{8\Sigma_{2s}}, \quad P_3 = -\frac{\Sigma_9}{4\Sigma_{2s}},$$

$$P'_4 = \frac{\Sigma_4}{\sqrt{-\Sigma_{2s}\Sigma_{2c}}}, \quad P'_5 = \frac{\Sigma_5}{2\sqrt{-\Sigma_{2s}\Sigma_{2c}}}, \quad P'_6 = -\frac{\Sigma_7}{2\sqrt{-\Sigma_{2s}\Sigma_{2c}}}.$$

These observables remain independent of each other when the leptons are assumed to be massless. As it was explained above, two more independent observables can be defined in case one lifts this assumption and incorporates lepton-mass dependent contributions to the decay rate. These other observables have some special features and we discuss them separately in Sec 4.2.3. Nevertheless, we keep all the lepton-masses at their physical values in the differential decay rate and, in particular, in the expressions of the angular coefficients.

The set of observables in Eqs. (85) is considered clean in the sense that the soft form factors cancel at LO in the ratios so that the uncertainty stemming from the form factors is suppressed in α_s (as computed at NLO in QCD factorization) or Λ/m_b (unknown factorizable power corrections). Notice that some of these observables can be related with others previously defined in the literature [32, 38, 53]. In order to form a complete set of independent observables, in the (pseudo)scalar-less case, we add the decay rate Γ' and F_L ,

$$\Gamma' = \frac{1}{2} \frac{d\Gamma + d\bar{\Gamma}}{dq^2} = \frac{1}{4} ((3\Sigma_{1c} - \Sigma_{2c}) + 2(3\Sigma_{1s} - \Sigma_{2s})) \quad (80)$$

$$F_T = \frac{3\Sigma_{1s} - \Sigma_{2s}}{2\Gamma'}, \quad F_L = \frac{3\Sigma_{1c} - \Sigma_{2c}}{4\Gamma'}, \quad (81)$$

satisfying $F_T = 1 - F_L$. Another option would involve, e.g., the forward-backward asymmetry (41) although notice that it can be obtained straightforwardly combining P_2 , F_L and the decay rate.

In Fig. 7 we plot the differential branching fraction, F_L and the clean observables $P_{1-6}^{(\prime)}$, and we follow the same color and line code as the one used in Fig. 6. Also, we show in black boxes the experimental results for the two first observables in the bins $[0.05, 2]$ GeV² and $[2, 4.3]$ GeV² that have been measured by the LHCb collaboration [6]. These measurements agree very well with the SM

predictions. By comparing the first row with the second and third rows of the panel in Fig. 7, we ratify the advantage of using a set of observables with reduced theoretical uncertainties [32, 57, 66]. While for the differential branching fraction and F_L the limited knowledge of the hadronic parameters (specially the soft form factors) is the dominant source of uncertainty, for the $P_i^{(\prime)}$ the power corrections become much more important. In the latter case, the enforcement of the form factor relations (44) is essential to constrain the size of the factorizable power corrections at very low q^2 , cf. P_1 and P_3 . As a consequence, the uncertainty in this region is dominated by the power corrections to the charm loop. This has to be interpreted as an outcome of the not-very-precise knowledge we have of these contributions, as compared with the information we can gather for the form factors. As for the effect of long-distance effects in the light-quark contributions we see that, indeed, they can modify abruptly the line shape of most of the observables in the neighborhood of the vector-resonance poles. Nevertheless, these effects are again tiny in P_1 and P_3 (which are $\propto H_{V,A}^+$) and, as argued in Sec. 3, they dilute after binning in q^2 . Moreover, P_1 and P_3 as pure helicity-1 objects are free from S -wave contamination. They emerge as especially clean null tests of the Standard Model.

On the experimental side [6], what is measured are ratios of binned observables (rather than binned ratios), hence it becomes necessary to define the observables not as q^2 -integrals of functions of the I_i 's but rather as the same functions of the corresponding binned angular coefficients; only in case the coefficients are slowly varying functions of q^2 in the bin considered, the two methods give approximately the same result. As one can deduce from Figs. 7 and 6, this *is not* the case around the low- q^2 end-point. With these considerations, we define the following set of CP-averaged binned observables [66],

$$\begin{aligned}
\langle \Gamma' \rangle &= \frac{1}{2} \left\langle \frac{d\Gamma + d\bar{\Gamma}}{dq^2} \right\rangle, & \langle F_L \rangle &= \frac{\langle 3\Sigma_{1c} - \Sigma_{2c} \rangle}{4\langle \Gamma' \rangle}, \\
\langle P_1 \rangle &= \frac{\langle \Sigma_3 \rangle}{2\langle \Sigma_{2s} \rangle}, & \langle P_2 \rangle &= \frac{\langle \Sigma_6 \rangle}{8\langle \Sigma_{2s} \rangle}, & \langle P_3 \rangle &= -\frac{\langle \Sigma_9 \rangle}{4\langle \Sigma_{2s} \rangle}, \\
\langle P_4' \rangle &= \frac{\langle \Sigma_4 \rangle}{\sqrt{-\langle \Sigma_{2s} \rangle \langle \Sigma_{2c} \rangle}}, & \langle P_5' \rangle &= \frac{\langle \Sigma_5 \rangle}{2\sqrt{-\langle \Sigma_{2s} \rangle \langle \Sigma_{2c} \rangle}}, & \langle P_6' \rangle &= -\frac{\langle \Sigma_7 \rangle}{2\sqrt{-\langle \Sigma_{2s} \rangle \langle \Sigma_{2c} \rangle}},
\end{aligned} \tag{82}$$

where $\langle \Sigma_i \rangle = \int_{q_{min}^2}^{q_{max}^2} \Sigma_i(q^2) dq^2$. In Table 3, we present the predictions for the binned observables, as defined in Eq. (82), in some bins of interest [111]. In particular, we highlight the results on the low- q^2 bin [0.1, 1] GeV², which presents an overall small theoretical (relative) error, as compared with the higher q^2 bins, due to the small form factor uncertainties in this region. It is also remarkable that the estimate on the contributions from the light hadronic resonances comes to

Table 3: Results and error budget on the binned CP-averaged observables of the muonic mode.

Obs.	$[q_{min}^2, q_{max}^2]$	Result	Hadronic	Fact.	c -quark	Light-quark
$10^7 \times \langle \frac{d\mathcal{B}}{dq^2} \rangle$	[0.1, 1]	$0.81^{+0.23}_{-0.20}$	+0.20 -0.17	+0.03 -0.03	+0.10 -0.10	± 0.00
	[0.1, 2]	$1.13^{+0.39}_{-0.38}$	+0.36 -0.24	+0.08 -0.07	+0.13 -0.12	± 0.02
	[2, 4.3]	$0.62^{+0.33}_{-0.26}$	+0.27 -0.21	+0.19 -0.15	+0.02 -0.01	± 0.00
	[1, 6]	$1.5^{+0.8}_{-0.6}$	+0.6 -0.5	+0.46 -0.37	+0.05 -0.05	± 0.02
$\langle F_L \rangle$	[0.1, 1]	$0.20^{+0.11}_{-0.10}$	+0.10 -0.09	+0.02 -0.02	+0.03 -0.02	± 0.01
	[0.1, 2]	$0.31^{+0.16}_{-0.12}$	+0.15 -0.11	+0.04 -0.04	+0.04 -0.03	± 0.01
	[2, 4.3]	$0.75^{+0.11}_{-0.16}$	+0.09 -0.13	+0.07 -0.9	+0.02 -0.02	± 0.00
	[1, 6]	$0.70^{+0.14}_{-0.17}$	+0.11 -0.13	+0.09 -0.11	+0.02 -0.02	± 0.00
$10^2 \times \langle P_1 \rangle$	[0.1, 1]	$2.9^{+3.2}_{-3.1}$	+0.8 -0.1	+1.2 -1.3	+2.9 -2.8	± 0.0
	[0.1, 2]	$3.0^{+3.5}_{-3.4}$	+0.8 -0.2	+1.7 -1.7	+2.9 -2.9	± 0.1
	[2, 4.3]	-1^{+7}_{-5}	+1.6 -0.8	+7 -5	+1.8 -1.6	± 0.0
	[1, 6]	-2^{+8}_{-6}	+1.3 -0.8	+8 -6	+1.6 -1.4	± 0.0
$10 \times \langle P_2 \rangle$	[0.1, 1]	$1.02^{+0.15}_{-0.17}$	+0.08 -0.13	+0.10 -0.09	+0.08 -0.07	± 0.00
	[0.1, 2]	$1.57^{+0.19}_{-0.26}$	+0.08 -0.20	+0.13 -0.13	+0.11 -0.10	± 0.04
	[2, 4.3]	$3.1^{+1.4}_{-1.6}$	+0.8 -0.8	+1.0 -1.2	+0.5 -0.7	± 0.0
	[1, 6]	$1.4^{+1.5}_{-1.5}$	+0.8 -0.7	+1.2 -1.1	+0.5 -0.6	± 0.0
$10^2 \times \langle P_3 \rangle$	[0.1, 1]	$-0.1^{+1.5}_{-1.2}$	+0.0 -0.2	+0.1 -0.1	+1.5 -1.2	± 0.0
	[0.1, 2]	$-0.2^{+1.6}_{-1.3}$	+0.0 -0.2	+0.1 -0.1	+1.6 -1.2	± 0.0
	[2, 4.3]	$-0.3^{+1.2}_{-1.2}$	+0.1 -0.3	+0.7 -0.8	+1.0 -0.9	± 0.0
	[1, 6]	$-0.3^{+1.0}_{-1.0}$	+0.1 -0.3	+0.6 -0.6	+0.8 -0.7	± 0.0
$10 \times \langle P'_4 \rangle$	[0.1, 1]	$-5.1^{+0.9}_{-0.4}$	+0.8 -0.0	+0.2 -0.2	+0.3 -0.2	± 0.3
	[0.1, 2]	$-3.8^{+1.4}_{-0.6}$	+1.2 -0.0	+0.3 -0.3	+0.4 -0.4	± 0.4
	[2, 4.3]	$4.6^{+1.8}_{-2.2}$	+0.9 -1.4	+1.3 -1.4	+1. -0.9	± 0.0
	[1, 6]	$4.6^{+1.6}_{-1.9}$	+0.9 -1.2	+1.1 -1.2	+0.8 -0.8	± 0.0
$10 \times \langle P'_5 \rangle$	[0.1, 1]	$6.9^{+0.8}_{-0.5}$	+0.6 -0.1	+0.3 -0.3	+0.2 -0.2	± 0.3
	[0.1, 2]	$5.5^{+0.7}_{-1.1}$	+0.1 -0.8	+0.6 -0.6	+0.3 -0.3	± 0.2
	[2, 4.3]	$-2.5^{+3.1}_{-2.7}$	+1.5 -1.1	+2.5 -2.3	+0.9 -1.0	± 0.0
	[1, 6]	$-2.8^{+3.0}_{-2.6}$	+1.3 -1.1	+2.5 -2.2	+0.8 -0.9	± 0.0
$10 \times \langle P'_6 \rangle$	[0.1, 1]	$-0.8^{+0.7}_{-0.8}$	+0.3 -0.4	+0.0 -0.0	+0.7 -0.7	± 0.0
	[0.1, 2]	$-0.8^{+0.7}_{-0.8}$	+0.2 -0.5	+0.0 -0.0	+0.7 -0.7	± 0.0
	[2, 4.3]	$-0.9^{+1.0}_{-1.0}$	+0.3 -0.5	+0.1 -0.1	+0.9 -0.9	± 0.0
	[1, 6]	$-0.7^{+0.8}_{-1.0}$	+0.2 -0.5	+0.1 -0.1	+0.8 -0.8	± 0.0

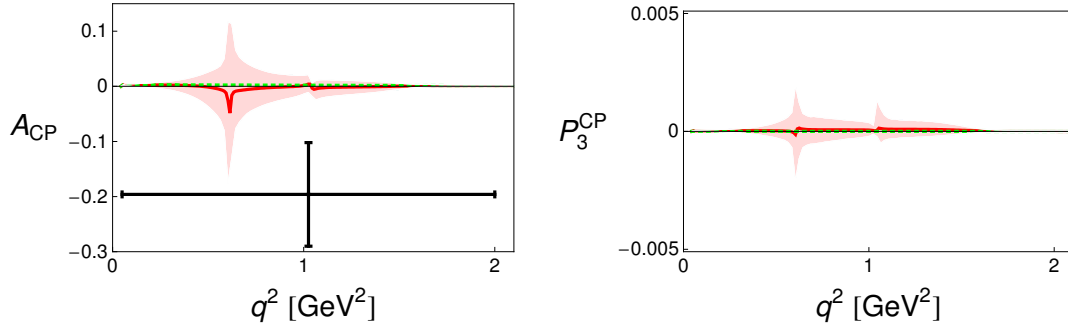


Figure 8: Differential A_{CP} and P_3^{CP} at low q^2 . For A_{CP} we show the experimental data point at the low- q^2 bin $[0.05, 2]$ GeV^2 . The charm-loop uncertainty and factorizable power corrections are negligible in this case.

be, for the CP averages, negligible. In this regard, the largest pollution appears in the bins including the $\phi(1020)$ resonance and in the observable P'_4 . As we will see in Sec. 4.4, low- q^2 bins are also important for their sensitivity to the Wilson coefficients C_7 and C'_7 .

4.2.2 CP asymmetries: A_{CP} and P_3^{CP}

The CP asymmetries are observables suitable for searching for sources of CP-violation beyond the CKM mechanism. In $\bar{B} \rightarrow \bar{K}^* \ell^+ \ell^-$, a weak phase arises from the interference between the contributions weighed by $V_{tb} V_{ts}^*$ and $V_{ub} V_{us}^*$, so all the CP-asymmetries for this decay in the SM are suppressed by a factor $\lambda_{ut} = V_{ub} V_{us}^* / V_{tb} V_{ts}^*$, which imaginary part is of order $\sim \bar{\eta} \lambda^2 \sim 10^{-2}$ [18]. Another important observation is that the sensitivity to a CP-violating phase is modulated by a factor $\sin \delta_s \sin \delta_w$ or $\cos \delta_s \sin \delta_w$ depending on whether the asymmetry is T-even or T-odd (i.e odd under the transformation $\phi \rightarrow -\phi$). In this sense, QCD factorization predicts the strong phases, δ_s , to be very small [23, 29] and, consequently, the latter asymmetries have been specifically singled out as interesting observables for the detection of new CP-violating phases beyond the SM [37].

Nonetheless, a hadronic, rather than a partonic treatment, is suited for the description of the contribution of the light-quarks at low- q^2 (see Sec. 3). In the context of VMD that is developed in this work, we have concluded that the overall contribution to the CP-averaged observables is negligible and consistent with the intrinsic suppression induced by small Wilson coefficients or by the CKM factor λ_{ut} . For the CP-asymmetries, though, large differences between the two approaches can be expected since the leading contribution is given by the latter pieces. To be more precise, large strong phases can be obtained in the hadronic picture as they naturally arise from rescattering and “dressing” of the resonance poles. Therefore, at low q^2 a suppression $\propto \sin \delta_s \approx 0$ of the T-even asymmetries

cannot be expected and sensitivity to the weak phase(s) in these observables can be generated by long-distance effects. Conversely, a factor $\cos \delta_s$ close to 1 is not guaranteed on general grounds at low q^2 , which can hinder the efficient use of the T-odd observables for probing CP-violation in this regime.⁸

As an illustration, we show in the left-hand side of Fig. 8 the CP-asymmetry

$$A_{\text{CP}} = \frac{\Gamma - \bar{\Gamma}}{\Gamma + \bar{\Gamma}} = \frac{3\Delta_{1c} - \Delta_{2c} + 2(3\Delta_{1s} - \Delta_{2s})}{4\Gamma'}, \quad (83)$$

which is T-even and, on the right hand-side, the T-odd asymmetry P_3^{CP} [112],

$$P_3^{\text{CP}} = -\frac{\Delta_9}{4\Sigma_{2s}}, \quad (84)$$

for the decays of the neutral mesons in the muonic mode. The latter observable is a redefinition of A_9 [18,39] following the same “cleanness” principle applied to set the P -basis for the CP-averaged observables [112]. A_{CP} has been measured at the B -factories [4,10] and, recently, binned results and the most precise measurement to date of the total have been provided by the LHCb collaboration [113]. An interesting outcome of the latter measurement is that the total (integrated) A_{CP} is negative and of order $\sim 5\%$, with a sizable and negative contribution stemming from the lowest- q^2 bin. This seems to be in contradiction, at 1σ level, with the SM prediction as it is obtained in QCD factorization. On the other hand, this type of substantial CP-asymmetries could be the smoking gun for some NPs scenarios (see e.g. [54]). However, and as shown in the left-hand side panel of Fig. 8 long-distance contributions of the light quarks can have an important effect in A_{CP} . In fact, we obtain that the uncertainty produced by these can be rather large, cf. $A_{\text{CP}} = (0_{-4}^{+3})\%$ in the $[0.05, 2]$ GeV^2 bin, with an error band one order of magnitude larger than in QCD factorization.

As for P_3^{CP} we observe that it is practically zero in the SM. This observable (in the form of A_9) has been tagged as a benchmark for the detection of a non-standard weak phase that might surface through the Wilson coefficient C'_7 [37,39], and our findings show that it remains a clean null test, safe from long-distance charm contributions and contamination by light resonances as a consequence of being $\propto H_{V,A}^+$. We investigate the sensitivity of this observable, together with other combinations of the angular coefficients I_3 and \bar{I}_3 , to BSM values of C'_7 , in Sec. 4.4.

⁸In any case, we want to stress that a full treatment of the hadronic uncertainties on the CP-asymmetries is beyond the scope of the present work. For instance, neglecting the effect of higher-mass ρ , ω and ϕ resonances present across all the lowest- q^2 region might not be as safe approximation for the CP-asymmetries as it is for the averages.

4.2.3 Non-vanishing lepton masses: The observables M_1 and M_2

Two more independent “clean” observables can be defined for the muonic mode at low q^2 [57],⁹

$$M'_1 = \frac{1}{1 - \beta^2} \frac{\beta^2 I_{1s} - (2 + \beta^2) I_{2s}}{4 I_{2s}}, \quad M'_2 = -\frac{1}{1 - \beta^2} \frac{\beta^2 I_{1c} + I_{2c}}{I_{2c}}, \quad (85)$$

which involve the pieces proportional to $4m_\mu^2/q^2$ present in I_{1s} and I_{1c} ,

$$\begin{aligned} M'_1 &= \frac{1}{2} \frac{(|H_V^+|^2 + |H_V^-|^2 - (V \rightarrow A))}{(|H_V^+|^2 + |H_V^-|^2 + (V \rightarrow A))}, \\ M'_2 &= \frac{q^2/(2m_\mu^2)(|H_P|^2 + \beta^2|H_S|^2) + (|H_V^0|^2 - |H_A^0|^2)}{(|H_V^0|^2 + |H_A^0|^2)}. \end{aligned} \quad (86)$$

The two questions that naturally arise are, first, what can we learn from a measurement of these observables; second, how these pieces enter in the formulas of the differential decay rate expressed in terms of a given basis of observables, which are usually defined in the $m_\ell \rightarrow 0$ limit. To start off, notice that the contribution of these pieces to the differential decay rate vanishes except in the vicinity of the low- q^2 end-point, e.g. $4m_\mu^2/(0.5\text{GeV}^2) \sim 0.09$. In this region it then follows that

$$M'_1 = \frac{1}{2} + \mathcal{O}(q^2/m_B^2)^2, \quad M'_2 = 1 + \mathcal{O}(q^2/m_B^2). \quad (87)$$

To obtain the first relation it is sufficient to note that the photon pole in H_V^\pm makes H_A^\pm to be of $\mathcal{O}(q^2/m_B^2)$ in comparison. Thus, this relation is completely model-independent, in the sense that it is insensitive to the long-range hadronic uncertainties as well as to the particular short-range structure of the decay. In order to derive the second relation, we first omit the effect of (pseudo)scalar operators. Then, using the corresponding expressions for the amplitudes it is straightforward to obtain

$$|H_V^0|^2 + q^2/(2m_\mu^2)|H_P|^2 - |H_A^0|^2 = |H_V^0|^2 + |H_A^0|^2 + \text{Rem.}, \quad (88)$$

where

$$\text{Rem.} = \frac{N^2 \lambda}{2m_B^2 q^2} |C_{10} - C'_{10}|^2 (S(q^2) - V_0(q^2)) \simeq \mathcal{O}(q^2/m_B^2) \quad (89)$$

due to the exact form-factor relation (45). The relation for M'_2 is not model-independent as it can be broken by contributions from BSM scalar and pseudoscalar operators, although the size of these effects is very constrained by recent

⁹For the sake of making our discussion in this section more transparent, we slightly redefine these observables as introduced in that reference, factorizing out a $4m_\mu^2/q^2$ piece.

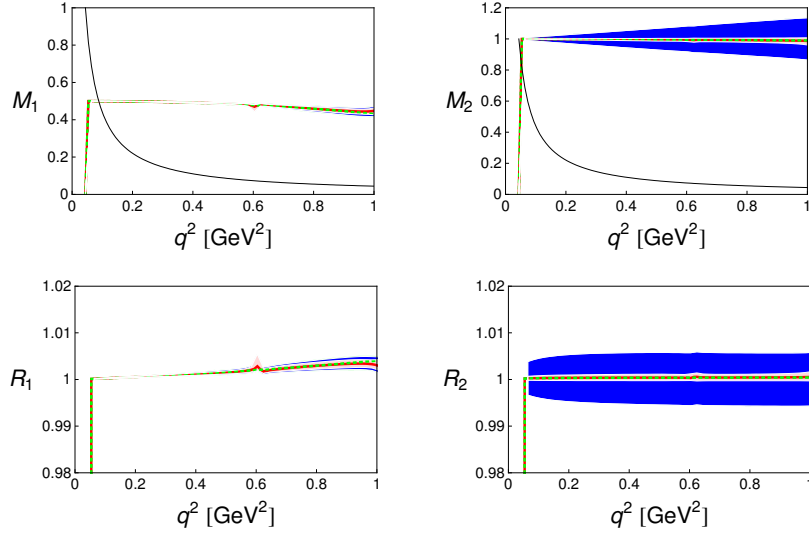


Figure 9: Results for $M'_{1,2}$ and $R_{1,2}$. The color code is as in Fig. 6, whereas the black line is the suppression factor $4m_\mu^2/q^2$.

measurements of the $B_s \rightarrow \mu^+ \mu^-$ decay rate. Indeed, if one uses the experimental upper bound given by the LHCb collaboration at 1- σ level [1] and the SM prediction in Ref. [2] to constrain the size of these pieces (assuming $C_{10} = C_{10}^{\text{SM}}$), one obtains that the relation for M'_2 is broken only at the $\sim 1\%$ level.

The Eqs. (87) mean that, in practice, $M'_{1,2}$ are not independent observables in the q^2 region in which the decay distribution has sensitivity to their effects. Taking this into account, one can generalize Eqs. (78) with expressions that are valid at finite m_ℓ and then, also, close to the low- q^2 end-point. Namely, we define,

$$\tilde{I}_{1s} = \frac{1}{\beta^2}(4 - \beta^2)I_{2s}, \quad \tilde{I}_{1c} = -\frac{1}{\beta^2}(2 - \beta^2)I_{2c}, \quad (90)$$

that convert into the conventional formulas (78) in the massless limit. In the upper panel of Fig. 9 we show the q^2 dependence of M'_1 and M'_2 at low q^2 using the same color code as in Figs. 6 and 7. We superimpose in black the value of the factor $4m_\mu/q^2$ suppressing the contribution of these pieces to the decay rate. In the lower panel we explore the validity Eqs. (90) by showing the ratios $R_{1,2} = \tilde{I}_{1s,2s}/I_{1s,2s}$. As one can check in the plots, these relations work at better than 1% of accuracy in the region of interest.

4.3 The $\bar{B}^0 \rightarrow \bar{K}^{*0} e^+ e^-$ decay

In comparison with the muonic mode, the electronic decay is interesting because its low- q^2 end-point is at $q^2 = 4m_e^2 \simeq 10^{-6}$ GeV². Hence, it presents an

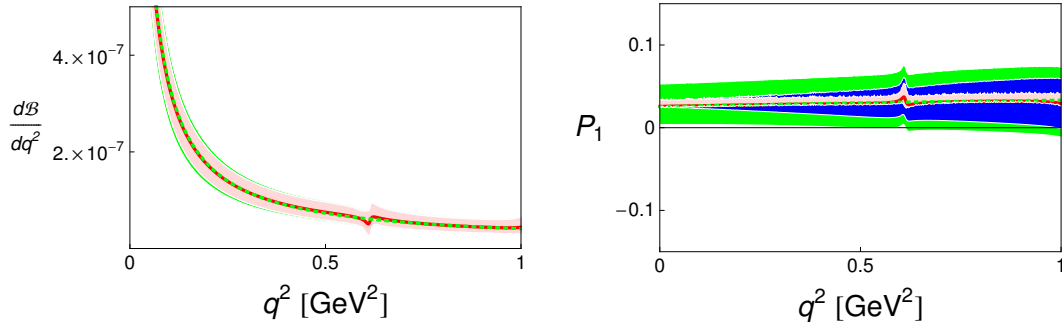


Figure 10: Differential branching fraction and P_1 for the electronic mode at low q^2 . The color code is as in Fig. 6.

Table 4: Results and error budget of the integrated branching fraction and P_1 observable in the $[0.0009, 1]$ GeV^2 bin for the electronic mode.

Obs.	Result	Hadronic	Fact.	c -quark	Light-quark
$10^7 \times \langle \frac{d\mathcal{B}}{dq^2} \rangle$	$2.43^{+0.66}_{-0.47}$	$+0.50$ -0.39	$+0.10$ -0.05	$+0.42$ -0.25	± 0.03
$10^2 \times \langle P_1 \rangle$	$2.7^{+3.0}_{-2.7}$	$+0.8$ -0.1	$+1.0$ -1.2	$+2.7$ -2.3	± 0.0

enhanced sensitivity to the physics associated to the photon pole becoming a golden mode for probing possible BSM effects related to the magnetic penguins operator $Q_7^{(f)}$ [21]. On the experimental side, B -factories have observed the electronic mode [10], and prospects at LHCb are discussed in [114]. This will also be an interesting target for super flavour factories. Our detailed error assessment of the low- q^2 region in the muonic mode revealed that the low- q^2 end-point is actually the least prone to form factors uncertainties due to the constraints (44), at the same time as the hadronic contributions, for CP-averaged observables, come out to be of negligible size. Consequently, the $\bar{B}^0 \rightarrow \bar{K}^{*0} e^+ e^-$ decay emerges as highly relevant.

In Fig. 10 we show the SM predictions for the differential branching fraction and the P_1 observable, which is especially sensitive to NPs effects in the magnetic penguin operators [32, 57]. In Table 4 we show the integrated results for the bin $[0.0009, 1]$ GeV^2 , that is the one proposed in [114]. As one can see, the integrated branching fraction is larger than the one for the muonic case in its lowest bin. Interestingly enough, our result agrees with the estimate $\mathcal{B} \sim 2.2 \times 10^{-7}$ that is obtained assuming that the decay is entirely driven by the photon pole [21, 114]. This dominance of the transverse amplitudes in this integrated decay rate is also reflected by a very small integrated longitudinal polarization in the same bin, namely $\langle F_L \rangle = 0.077^{+0.047}_{-0.040}$.

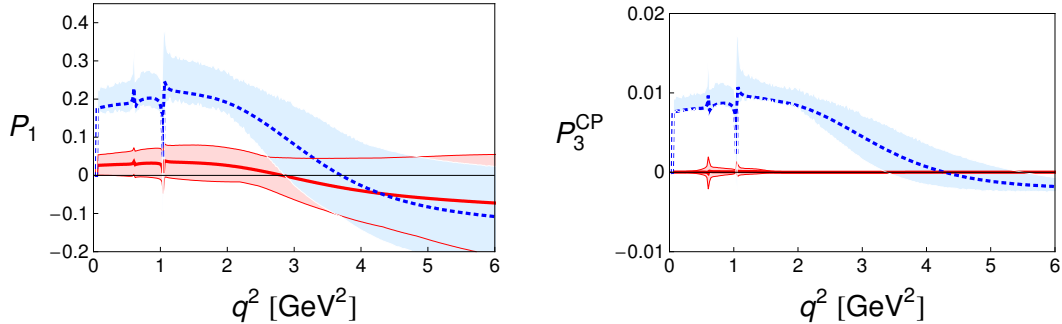


Figure 11: Study of the sensitivity of the observables P_1 and P_3^{CP} to the a purely real or purely imaginary NPs contribution through C'_7 (dashed line, blue bands). These are confronted with the SM expectation (solid line, red band).

4.4 Sensitivity to C'_7

The analysis of the low q^2 region of the $\bar{B} \rightarrow \bar{K}^* \ell^+ \ell^-$ can provide tight constraints on NPs scenarios with right-handed flavour-changing neutral currents, specially those giving contributions to the chirally-flipped magnetic penguin operator \mathcal{O}'_7 . This is due to the fact that the angular coefficients I_3 and I_9 , at low- q^2 , are

$$I_3 \propto \text{Re}(H_V^- H_V^{+*}), \quad I_9 \propto \text{Im}(H_V^- H_V^{+*}), \quad (91)$$

where $H_V^+ \propto C'_7/q^2$, so, approximately, they vanish unless $C'_7 \neq 0$. (Corrections involving H_A^+ are also suppressed by the smallness of C'_9 and C'_{10} in the Standard Model, but any BSM effects generating H_A^+ are suppressed at $q^2 \approx 0$ due to the absence of a photon pole.) In the SM, small contributions to these observables are generated by the strange-quark mass and other effects quantified in this work as contributions to the H_V^+ helicity amplitude. Other decays and observables provide valuable and independent constraints on the C_7 and the C'_7 planes, in particular the inclusive $B \rightarrow X_s \gamma$ decay and the isospin and the time-dependent CP-asymmetries in the exclusive $B \rightarrow K^* \gamma$ decay (see e.g. [64]). The interest of the radiative decays onto higher-mass K^* resonances has been also recently pointed out [48]. In this work we focus on studying the sensitivity of the vicinity of low- q^2 end-point to the chirally-flipped Wilson coefficient C'_7 . A more comprehensive analysis should also consider studying new-physics effects in C_7 [63–65], although I_3 and I_9 can be used to efficiently constrain also this Wilson coefficient only if C'_7 is far from zero.

In the context of CP-combinations, one can construct 4 independent observables with these angular coefficients and their CP-conjugates. However, I_3 and I_9 are a CP-odd and a CP-even observable, respectively, and the combinations Δ_3 and Σ_9 become not very sensitive to the chirality of dilepton pair. Therefore, only 1 CP-average and 1 CP-asymmetry, constructed from Σ_3 and Δ_9 , in order, are

sensitive to either the real or imaginary parts of $C_7^{(\prime)}$. The corresponding observables in the P -basis, P_1 and P_3^{CP} , are a convenient choice for their intrinsically reduced theoretical uncertainty. In order to investigate the sensitivity of these observables to $C_7^{(\prime)}$, we investigate two a priori fictitious scenarios: the first one in which $C_7^{(\prime)}$ is real and with a magnitude of 10% the value of $C_7(m_b)$ in the SM, and second where $C_7^{(\prime)}$ is a pure imaginary number with an absolute value of 1% the value of $C_7(m_b)$ in the SM. The result for P_1 in the first scenario is plotted as a dashed line confronted against the SM prediction represented as a solid line on the left panel of 11. The corresponding bands are the overall uncertainties in these scenarios calculated as those presented for the SM in the previous sections. On the right-hand side, we plot P_3^{CP} for the second scenario compared, again, with the SM prediction and following the same line and color code as on the left panel.

The first remarkable outcome of this analysis is that, with the current theoretical uncertainties, P_1 is sensitive to a $C_7^{(\prime)}$ with a real part of about $10\% \times C_7^{\text{SM}}(m_b)$ only in the region between $q^2 = 4m_\ell^2$ and $q^2 \simeq 3 \text{ GeV}^2$. The same conclusions apply to P_3^{CP} although, in this case, the attainable accuracy is much higher as it can be sensitive to complex phases with an absolute value below $1\% \times C_7^{\text{SM}}(m_b)$. This, in principle, is an important result as it singles out P_3^{CP} as a theoretically extremely clean observable to constrain (or favor) BSMs generating new CP-violating phases through $C_7^{(\prime)}$. This occurs despite the cautionary remarks made in Sec. 4.2.2 about the CP-asymmetries. In fact important interference with strong phases, with a drastic reduction of the sensitivity, seems to appear only in the immediate surroundings of the resonance poles. Notice, however, that P_3^{CP} is a special observable as it vanishes in the SM so the cleanness of other CP-observables can not be concluded without a devoted study on their corresponding hadronic uncertainties.

5 Conclusions and outlook

We have performed a comprehensive analysis of angular observables in the decays $\bar{B} \rightarrow \bar{K}^* \ell^+ \ell^-$, $\ell = \mu, e$, paying particular attention to non-factorizable hadronic uncertainties. We exploit a suppression of the positive-helicity amplitudes in the Standard Model that, as we have shown, still holds when taking into account long-distance charm and light-quark non-factorizable effects in a conservative way. As a result, we established that of those observables that are “clean” in the factorizable approximation in the large-energy/heavy-quark limit, the two observables $P_1 = A_T^{(2)}$ and P_3^{CP} are found to nearly vanish in the SM with very small errors in the presence of the long-distance non-factorizable corrections. At the same time they are highly sensitive to right-handed currents. Importantly, we find that the lower end of the low- q^2 range is not only theoretically clean, but provides the best sensitivity to the Wilson coefficient $C_7^{(\prime)}$, down to a (theoretical)

limit of below 10% for the real part, and as low as 1% for the imaginary part. This also raises the profile of the decay into electrons, $\ell = e$, which is dominated by the photon pole, due to the small electron mass. We feel that this process deserves further attention. For other observables, which do not vanish for $H_V^+ = 0$, the theoretical control is more compromised by long-distance effects. Improving it would seem to require further theoretical advances.

As a further result, we have found a way to generalise the two well-known relations $3I_{1s} = I_{2s}$ and $I_{1c} = -I_{2c}$, which hold for vanishing lepton mass, to the massive case. This may be of use in the experimental determination of the angular distribution.

The formulation in terms of helicity amplitudes allowed us to show, by adapting the LCSR formalism of [46], a strong $\Lambda^3/(4m_c^2 m_b)$ power suppression of the long-distance contribution $h_+|_{c\bar{c},\text{LD}}$ from the charm part of the hadronic weak Hamiltonian entering in the positive-helicity amplitude H_V^+ , which vanishes at leading power in QCDF. Analogous contributions from the chromomagnetic operator are suppressed by Λ^2/m_b^2 . Likewise, we exclude the possibility of non-negligible, light-resonance long-distance contributions to H_V^+ once the $(\Lambda/m_b)^2$ suppression of the corresponding $\bar{B} \rightarrow \bar{K}^*V$ helicity amplitude is taken into account. More generally, we observe that, once data are binned, these light-resonance contributions are small in all observables, even though this is not true of the unbinned quantities. On the other hand, the amplitudes H_V^- and H_V^0 can receive important long-distance charm-loop contributions, at a level of $\mathcal{O}(10\%)$ of the leading-power QCDF result, as is clear from the numerical values in [46]. We have also argued that the much smaller estimate of these contributions of [34] is likely to suffer very large, incalculable corrections. This limits the theoretical control over the other “clean” observables, beyond P_1 , P_3 , and their CP asymmetry counterparts, that, although independent of H_V^0 , involve H_V^- .

Our phenomenological analysis makes certain assumptions about the values of helicity form factors and nonfactorizable corrections to the helicity amplitudes. To get a better quantitative understanding of the theoretical errors, it would be desirable to have direct calculations of form factors in the helicity basis. This should be straightforward within LCSR, or other methods. It is also important to stress that we have not derived a sum rule for $h_+|_{c\bar{c},\text{LD}}$, but only shown a parametric suppression of it (and of the Q_{8g} long-distance contributions.) An attractive aspect of the LCSR method is that it avoids endpoint divergences altogether, and a sum rule allowing for a quantitative estimate could in principle be obtained. We feel that that is a path worthwhile pursuing. On the other hand, for the light-quark non-factorizable effects it would be interesting to go beyond the resonance model in assessing the size (and helicity structure) of possible corrections to the QCDF results, perhaps by combining QCDF, LCSR, and dispersion relations along the lines of [94]. While this is unlikely to have a strong impact on P_1 or P_3^{CP} , it may be more important in other observables, and in particular for the direct CP asymmetry A_{CP} , which, as our resonance model suggests, could be

relatively sensitive to any large, “soft” strong phases associated with light-hadron intermediate states.

Acknowledgment. We would like to thank M. Beneke, C. Bobeth, U. Egede, G. Hiller, J. Matias, M. Patel, M.-H. Schune, N. Serra, R. Zwicky, and the participants of the *Workshop on the physics reach of rare exclusive B decays* held at Sussex in September 2012, for useful discussions. This work was funded by the UK Science and Technology Facilities Council under grant numbers ST/H004661/1 and ST/J000477/1. Support from SEPnet and NExT is acknowledged. JMC acknowledges partial support from the Spanish Ministerio de Economía y Competitividad and European FEDER funds under the contract FIS2011-28853-C02-01 and the Fundación Seneca project 11871/PI/09.

Note added. After submission of this work to the arXiv, a paper including a new LCSR approach to the matrix elements of Q_{8g} appeared [122]. It would be interesting to adapt this method to the approach of the present paper. We also note work on the effect of tensor operators in $\bar{B} \rightarrow K^* \ell^+ \ell^-$ in the high- q^2 region [123].

A Notations and conventions

A.1 Polarisation vectors

For a particle moving in $+z$ direction with four-momentum $k^\mu = (E, 0, 0, |\mathbf{k}|)$ we use

$$\epsilon_t^\mu = \frac{k^\mu}{\sqrt{k^2}}, \quad (92)$$

$$\epsilon^\mu(\pm) = \frac{1}{\sqrt{2}}(0, \mp 1, -i, 0), \quad (93)$$

$$\epsilon^\mu(0) = \frac{1}{\sqrt{k^2}}(|\mathbf{k}|, 0, 0, E). \quad (94)$$

In parentheses is the helicity, we sometimes alternatively put this in a subscript. The subscript t denotes “timelike” polarisation, which is a spin singlet. The sign conventions ensure that the helicities $\pm, 0$ form a triplet obeying conventional relative signs and normalisations, e.g. $[J^+]^\mu_\nu \epsilon^\nu(0) = \sqrt{2} \epsilon^\mu(1)$.

The polarisation vectors satisfy the normalisation and completeness relations

$$\epsilon_a^\mu \epsilon_{b,\mu}^* = g_{ab}, \quad g_{ab} = \begin{cases} -1, & a = b = \pm, 0, \\ 1, & a = b = t, \\ 0, & \text{otherwise} \end{cases} \quad (95)$$

$$\eta^{\mu\nu} = \epsilon_t^\mu \epsilon_t^{\nu*} - \sum_{\lambda=\pm,0} \epsilon^\mu(\lambda) \epsilon^{\nu*}(\lambda) = \sum_{a,b=t,\pm,0} g_{ab} \epsilon_a^\mu \epsilon_b^\nu. \quad (96)$$

For any other direction \hat{n} , we define the polarization vectors by applying a standard rotation after boosting to the “rest frame” where $k^\mu = (\sqrt{k^2}, 0, 0, 0)$. In that frame,

$$\epsilon^\mu(\hat{n}; \lambda) = \left[e^{-i\phi J_z} e^{-i\theta J_y} e^{+i\phi J_z} \right]^\mu{}_\nu \epsilon^\nu(\hat{z}; \lambda) = \sum_{\lambda'} d_{\lambda'\lambda}^1(\theta) e^{i(\lambda-\lambda')\phi} \epsilon^\mu(\hat{z}; \lambda'), \quad (97)$$

where θ, ϕ are the spherical coordinates of \hat{n} and $d_{m'm}^j(\theta)$ is the matrix element of the rotation operator $e^{-i\theta J_y}$ (conventions as in [115]). For arbitrary direction, the final form is usually more convenient.

For $\hat{n} = -\hat{z}$ (ie $\theta = \pi$) we rotate at $\phi = 0$. This means

$$\epsilon(-\hat{z}; \pm) = \epsilon(\hat{z}; \mp), \quad \epsilon(-\hat{z}; 0) = -\epsilon(\hat{z}; 0).$$

Boosting back to the laboratory frame, we have

$$\epsilon_t^\mu(-\hat{z}) = \frac{1}{\sqrt{k^2}} (E, 0, 0, -|\mathbf{k}|), \quad (98)$$

$$\epsilon^\mu(-\hat{z}; \pm) = \frac{1}{\sqrt{2}} (0, \pm 1, -i, 0) = \epsilon^\mu(\hat{z}; \mp), \quad (99)$$

$$\epsilon^\mu(-\hat{z}; 0) = \frac{1}{\sqrt{k^2}} (|\mathbf{k}|, 0, 0, -E). \quad (100)$$

A.2 Standard Model parameters

Table 5: Some of the SM parameters used in this work (in GeV).

M_W	$\hat{m}_t(\hat{m}_t)$	$m_{b,\text{PS}}$	m_c	$\hat{m}_s(2 \text{ GeV})$	$\Lambda_{\text{QCD}}^{(5)}$
80.4	172(2)	4.8(2)	1.3(1)	0.094(3)	0.214(8)

Table 6: CKM parameters in the Wolfenstein parameterization used in this work [116].

λ	A	$\bar{\rho}$	$\bar{\eta}$
0.22543(8)	0.805(20)	0.144(25)	0.342(16)

We use the PS-subtracted definition for the b -quark mass [23]. This is obtained from the $\overline{\text{MS}}$ -definition (\hat{m}_b) through the pole mass definition (m_b) using the subsequent identities

$$\hat{m}_b(\mu) = m_b \left(1 + \frac{\alpha_s(\mu) C_F}{4\pi} \left[3 \log \frac{m_b^2}{\mu^2} - 4 \right] + \mathcal{O}(\alpha_s^2) \right), \quad (101)$$

$$m_b = m_{b,\text{PS}}(\mu_f) + \frac{4\alpha_s(\mu)}{3\pi} \mu_f. \quad (102)$$

Table 7: Wilson coefficients of the SM at $\mu = 4.8$ GeV, in the basis of [73] and to NNLL accuracy.

C_1	C_2	C_3	C_4	C_5	C_6	C_7^{eff}	C_8^{eff}	C_9	C_{10}
-0.144	1.060	0.011	-0.034	0.010	-0.040	-0.305	-0.168	4.24	-4.312

The PS-mass at $\mu_f = 2$ GeV is then identified with the pole mass, $m_b \approx m_{b,\text{PS}}(2 \text{ GeV}) = 4.78_{-0.07}^{+0.20} \simeq 4.8(2)$ GeV [117]. We use m_b as the potential-subtracted definition unless it is stated otherwise. For the strange quark mass appearing at tree level we use the result obtained from LQCD calculations, $\hat{m}_s(2 \text{ GeV}) = 94(3)$ MeV [118]. Other SM parameters used in the calculation are listed in Tables 5 and 6. For $\alpha_s(\mu)$ we use the three-loop renormalization-scale evolution [119], for $\alpha_{\text{em}}(Q^2 = 0) \simeq 1/137$ and for $G_F = 1.16637(1) \times 10^{-5} \text{ GeV}^{-2}$. Finally, we show in Table 7 the values of the Wilson coefficients of the SM at $\mu = m_b$ GeV, in the basis of [73] and to NNLL accuracy.

A.3 Leading-twist LCDAs

We use the parameterization of the light vector-meson LCDAs of Ref. [77] in terms of the wave functions $\Phi_{K^*,a}(u)$ and the semileptonic decay constants. However, we use the conventions and values of Refs. [29], which have a sign difference in the odd-coefficients as compared with those of the LCSR calculation. Namely,

$$\Phi_{K^*,a} = 6u\bar{u} \left(1 + 3a_{1,a}\xi + a_{2,a}\frac{3}{2}(5\xi^2 - 1) \right), \quad (103)$$

with $\bar{u} = (1-u)$, $\xi = 2u-1$ and $a_{i,a}$ Gegenbauer coefficients. There are two decay constants for a light vector meson. The longitudinal constant can be obtained from experiment using the branching fractions for the electromagnetic decays of the neutral vector resonances and applying $SU(3)_F$ symmetry. We obtain $f_{K^*} = 220(5)$ MeV using the ρ decay and so this value is consistent with the one obtained from sum-rule calculations [77]. Sum rules also predict the tensor (transversal) decay constant, $f_{K^*,\perp}(1 \text{ GeV}) = 170(20)$ MeV. The latter is consistent with the LCSR determination $f_{K^*,\perp}(2 \text{ GeV}) \approx 160$ MeV [39], although we have considerably increased the uncertainty. We evolve the transversal constant in the renormalization scale as

$$f_{K^*,\perp}(\mu) = f_{K^*,\perp}(\mu_0) \left(\frac{\alpha_s(\mu)}{\alpha_s(\mu_0)} \right)^{4/23}. \quad (104)$$

For the B -meson, only two ‘‘moments’’ are needed,

$$\lambda_{B,+}^{-1} = \int_0^\infty d\omega \frac{\Phi_{B,+}(\omega)}{\omega}, \quad (105)$$

$$\lambda_{B,-}^{-1}(q^2) = \int_0^\infty d\omega \frac{m_B \Phi_{B,-}(\omega)}{m_B \omega - q^2 - i\epsilon}. \quad (106)$$

The wave functions $\Phi_{B,\pm}(\omega)$ are modelled such that they fulfill certain relations derived from the equations of motion [23, 71]. An important property is that $\lambda_{B,-}^{-1}(q^2)$ diverges logarithmically as $q^2 \rightarrow 0$,

$$\lambda_{B,-}^{-1}(q^2) \xrightarrow{q^2 \rightarrow 0} \infty, \quad (107)$$

However, this IR divergence only afflicts the longitudinal (helicity-zero) part of the decay amplitude, for which it indicates an enhanced long-distance sensitivity at low q^2 . The model employed in Ref. [23, 71] leads to the following expressions for the B -meson moments:

$$\lambda_{B,+}^{-1} = 1/\omega_0, \quad (108)$$

$$\lambda_{B,-}^{-1}(q^2) = \frac{\exp(-q^2/(m_B\omega_0))}{\omega_0} (-\text{Ei}(q^2/(m_B\omega_0)) + i\pi), \quad (109)$$

where $\omega_0 = 0.5(1)$ GeV. For f_B , we use an average of the current LQCD values with a generous error bar covering all of them $f_B = 190(20)$ MeV [120]. In Table 8 we collect the numerical values for the hadronic parameters used in this work.

Table 8: Summary of the K^* and B parameters used in this work.

f_{K^*}	$f_{K^*,\perp}$ (1 GeV)	$a_{1,a}$	$a_{2,a}$	f_B	$\lambda_{B,+}^{-1}$
220(5) MeV	170(20) MeV	0.2(2)	0.1(3)	190(20) MeV	2.0(5) GeV ⁻¹

A.4 Form factors

V denotes a vector meson, λ its helicity, ϵ_λ the corresponding polarization vector, etc. B is one of B^+ , B^0 , B_s . $q = p - k$.

$$\langle V(k, \lambda) | \bar{q} \gamma_\mu b | B(p) \rangle = \epsilon_{\mu\nu\rho\sigma} \epsilon_\lambda^{*\nu} p^\rho k^\sigma \frac{2}{m_B + m_V} V(q^2), \quad (110)$$

$$\begin{aligned} \langle V(k, \lambda) | \bar{q} \gamma_\mu \gamma_5 b | B(p) \rangle &= i(\epsilon_\lambda^* \cdot q) \frac{q_\mu}{q^2} 2 m_V A_0(q^2) \\ &+ i(m_B + m_V) \left(\epsilon_\lambda^{*\mu} - \frac{(\epsilon_\lambda^* \cdot q) q^\mu}{q^2} \right) A_1(q^2) \\ &- i(\epsilon_\lambda^* \cdot q) \left(\frac{(2p - q)^\mu}{m_B + m_V} - (m_B - m_V) \frac{q^\mu}{q^2} \right) A_2(q^2) \end{aligned} \quad (111)$$

$$q^\nu \langle V(k, \lambda) | \bar{q} \sigma_{\mu\nu} b | B(p) \rangle = 2i \epsilon_{\mu\nu\rho\sigma} \epsilon_\lambda^{*\nu} p^\rho k^\sigma T_1(q^2), \quad (112)$$

$$\begin{aligned} q^\nu \langle V(k, \lambda) | \bar{q} \sigma_{\mu\nu} \gamma_5 b | B(p) \rangle &= (\epsilon_{\lambda;\mu}^* (m_B^2 - m_V^2) - (\epsilon^* \cdot q)(2p - q)_\mu) T_2(q^2) \\ &+ (\epsilon^* \cdot q) \left(q_\mu - \frac{q^2}{m_B^2 - m_V^2} (2p - q)_\mu \right) T_3(q^2). \end{aligned} \quad (113)$$

The matrix element of the scalar density $\bar{q}b$ vanishes by parity. Furthermore, by PCAC,

$$i\langle V(k, \lambda) | \bar{q}\gamma_5 b | B(p) \rangle = \frac{2m_V}{m_b + m_q} (\epsilon^* \cdot q) A_0(q^2), \quad (114)$$

$$\langle V(k, \lambda) | \bar{q}P_{L,R} b | B(p) \rangle = \mp i \frac{m_V}{m_b + m_q} (\epsilon^* \cdot q) A_0(q^2). \quad (115)$$

Our sign convention for the Levi-Civita symbol is that of Bjorken and Drell, $\epsilon_{0123} = +1$. Our conventions agree with those of [39]. Some authors, in particular [23], agree on the physical meaning of the form factor symbols (in particular their signs), but differ in phase conventions for the hadron states, such that the form factor decompositions look different.

B Effective Lagrangian with vector resonances

We use the anti-symmetric representation of the vector-meson fields. We explain here the particular conventions used in the model and we show some of the results for its contribution to the amplitude. Further details on the anti-symmetric description of the spin-1 fields can be found in Ref. [97] whereas a discussion on the equivalence of this representation with any other one consistent with the symmetries and asymptotic behavior of QCD, can be found in Ref. [98]. We describe the $SU(3)$ -multiplets of resonances using flavor-matrices of anti-symmetric tensor fields (e.g. $V_{\mu\nu}$ for the nonet of vectors). The interaction Lagrangian for resonances [97,98], at leading order of the chiral expansion in the light sector, is

$$\mathcal{L}_V^{(2)} = \frac{f_V}{4} \langle V^{\mu\nu} F_{\mu\nu}^+ \rangle + i \frac{g_V}{2} \langle V^{\mu\nu} u_\mu u_\nu \rangle. \quad (116)$$

In this Lagrangian, u_ν is the *vielbein* introducing the pseudoscalar mesons (π , K , η_8) chirally coupled to the resonances fields and $F_{\mu\nu}^+$ is a generalized external-vector (electromagnetic) field strength, that in our case is $F_{\mu\nu}^+ \simeq 2eQF_{\mu\nu}$, with Q the charge operator in $SU(3)_F$ -space. The respective pieces come accompanied by the coupling constants f_V and g_V , which are defined in the chiral limit (the same as the mass term in the kinetic Lagrangian). The fields are normalized such that

$$\langle 0 | V^{\mu\nu} | V(p) \rangle = i m_V^{-1} (p^\mu \epsilon^\nu(p) - p^\nu \epsilon^\mu(p)). \quad (117)$$

so the vector-resonance fields have the same convention as the one employed in the definition of the form factors (see Sec. A.4). Finally, $V_{\mu\nu}$ includes the ω and ϕ mesons in ideal mixing,

$$\omega = \frac{1}{\sqrt{2}} (\bar{u}u + \bar{d}d), \quad \phi = \bar{s}s. \quad (118)$$

In the present case, we need only to consider the LHS of the Lagrangian in Eq. (116), with the effective coupling f_V receiving small $SU(3)_F$ corrections. We fix f_V for each resonance using the measured $V \rightarrow e^+e^-$ decay ratios. An explicit calculation shows that the decay amplitude of an on-shell resonance V with polarization λ into an electron (positron) with momentum q_- (q_+) and polarization s (s') is

$$\mathcal{M}_{V \rightarrow e^+e^-} = i \frac{e^2 f_V Q_V}{m_V} \left(g^{\mu\nu} - \frac{q^\mu q^\nu}{m_V^2} \right) \bar{u}(q_-, s) \gamma_\mu v(q_+, s') \epsilon_\nu(\lambda), \quad (119)$$

where Q_V depends on the charge of the constituent quarks in V , $Q_{\rho_0} = 1/\sqrt{2}$, $Q_\omega = 1/3\sqrt{2}$ and $Q_\phi = -1/3$, giving

$$\bar{\Gamma}_{V \rightarrow e^+e^-} = \frac{4\pi\alpha^2 f_V^2 Q_V^2}{3m_V}. \quad (120)$$

In Table 9 we list the effective parameters necessary for the description of the light-resonance propagation and decay, namely the masses, the decay width, the branching fraction for the $V \rightarrow e^+e^-$ decay and the values of f_V . For the latter, we obtain the errors summing up in quadrature those of the parameters propagated linearly through Eq. (120). We have also implemented the $SU(3)_F$ -breaking explicitly in the meson masses by using the measured Breit-Wigner values [117].

Table 9: Hadronic parameters of the light and neutral meson resonances.

V	m_V [MeV]	$\bar{\Gamma}_V$ [MeV]	$\mathcal{B}_{V \rightarrow e^+e^-} \times 10^{-5}$	f_V [MeV]
ρ_0	775.49(34)	149.1(8)	4.72(5)	221(1)
ω	782.65(12)	8.49(8)	7.28(14)	198(2)
ϕ	1019.455(20)	4.26(4)	29.54(30)	228(2)

On the other hand, the $\bar{B} \rightarrow V \bar{K}^*$ decay amplitude can be written as

$$\mathcal{M}_{\bar{B} \rightarrow V \bar{K}^*} = \epsilon_V^{*\mu} \epsilon_{K^*}^{*\nu} \mathcal{M}_{\mu\nu}^V, \quad (121)$$

and the contribution of the resonances to the decay is then

$$\mathcal{M}_{\bar{B} \rightarrow V(\rightarrow \ell^+ \ell^-) \bar{K}^*} = \frac{4\pi\alpha_{em} f_V Q_V}{m_V (q^2 - m_V^2 + im_V \Gamma_V)} \mathcal{M}_{\mu\nu}^V (\bar{\ell} \gamma^\mu \ell) \epsilon_{K^*}^{*\nu}, \quad (122)$$

where we ignore the off-shell dependence of the real and imaginary parts of the pole position and of the $\bar{B} \rightarrow V \bar{K}^*$ amplitude, all of which we expect to have a negligible effect. The decay amplitude in Eq. (121) is usually parameterized in terms of the three helicity amplitudes $H_V^{0,\pm} \propto \epsilon_V^{*\mu}(0, \pm) \epsilon_{K^*}^{*\nu}(0, \pm) \mathcal{M}_{\mu\nu}^V$ [107]. In principle, 5 different independent observables of the non-leptonic decay are required to extract, up to a global phase, the real and complex parts of these

Table 10: Results for the $\bar{B} \rightarrow V\bar{K}^*$ helicity amplitudes and on the relevant observables, which are compared to experimental data [121].

	ρ_0		ω		ϕ	
	Theo.	Expt.	Theo.	Expt.	Theo.	Expt.
$\mathcal{B} \times 10^6$	2.7(1.2)	3.9(0.8)	3.3(1.4)	2.0(5)	9.4(3.8)	9.8(0.7)
F_L [%]	31(20)	40(14)	53(20)	70(13)	59(19)	48(3)
ϕ_{\parallel} [°]	160(40)	–	120(31)	–	139(20)	136(8)
A_{CP}	–0.11(11)	–0.06(9)	14(15)	0.45(25)	0	0.01(5)

amplitudes. One takes the decay rate plus two out of three polarization fractions, f_L , f_{\perp} , f_{\parallel} , and two phases, ϕ_{\perp} , ϕ_{\parallel} ,

$$\Gamma = \frac{1}{16m_B\pi} (|A_0|^2 + |A_{\perp}|^2 + |A_{\parallel}|^2), \quad (123)$$

$$F_{L,\perp,\parallel} = \frac{|A_{0,\perp,\parallel}|^2}{|A_0|^2 + |A_{\perp}|^2 + |A_{\parallel}|^2}, \quad (124)$$

$$\phi_{\perp,\parallel} = \arg \frac{A_{\perp,\parallel}}{A_0}, \quad (125)$$

where we have used the transversity basis for the amplitudes¹⁰. Not all the amplitudes are equally important and in fact, in naive factorization, there exists a hierarchy among them,

$$H_V^0 : H_V^- : H_V^+ = 1 : \frac{\Lambda}{m_b} : \left(\frac{\Lambda}{m_b}\right)^2, \quad (126)$$

which results from the $V - A$ nature of the weak interactions and the approximate chiral-symmetry of the strong interactions at high energies. However, H_V^- does not factorize in QCDF, although nonfactorizable corrections have been estimated (including modelling of end-point-divergent convolutions) and found to be large, such that H_V^- can be comparable to H_V^0 . No factorization formula for H_V^+ is known, but for $\bar{B}^0 \rightarrow \phi\bar{K}^{*0}$ it has been extracted from experiment and found to be small, consistent with zero. This reduces to 3 the number of independent observables needed for the description of these non-leptonic decays. We summarize in the following the results for the two relevant amplitudes H_V^0 and H_V^- in QCD factorization [107] and we choose a normalization of the different pieces involved that makes the comparison with the other contributions to the semileptonic decay more transparent. We also discuss the corresponding predictions for the decay rate, F_L , ϕ_{\parallel} and A_{CP} compared to experimental data.

¹⁰We use a different sign convention for the definition of the transversal amplitude A_{\perp} as compared with Ref. [107].

The different amplitudes can be written as a sum of products of CKM matrix elements, factorizable coefficients containing form factors and decay constants and flavor amplitudes containing Wilson coefficients and perturbative corrections in the heavy quark limit. In case of the decays under study, we have [107]

$$\begin{aligned}
H_{\bar{B} \rightarrow \rho_0 \bar{K}^{*0}} &= -\frac{m_B}{\sqrt{2}} \sum_{p=c,u} \frac{\lambda_p}{\lambda_t} \left(A_{\rho \bar{K}^*} \hat{\alpha}_4^p - A_{\bar{K}^* \rho} \left(\frac{3}{2} \alpha_{3,\text{EW}}^p + \delta_{pu} \alpha_2 \right) \right), \\
H_{\bar{B} \rightarrow \omega \bar{K}^{*0}} &= \frac{m_B}{\sqrt{2}} \sum_{p=c,u} \frac{\lambda_p}{\lambda_t} (A_{\bar{K}^* \omega} (2\alpha_3^p + \delta_{pu} \alpha_2) + A_{\omega \bar{K}^*} \hat{\alpha}_4^p), \\
H_{\bar{B} \rightarrow \phi \bar{K}^{*0}} &= m_B A_{\bar{K}^* \phi} \frac{\lambda_c}{\lambda_t} (\hat{\alpha}_4^c + \alpha_3^c), \tag{127}
\end{aligned}$$

where $\lambda_i = V_{ib} V_{is}^*$ and we have omitted the polarization index. The values for the amplitudes $\alpha_i^{(p)}$, $\beta_i^{(p)}$ and $\hat{\alpha}_4$ that we use are listed in Table 2 of Ref. [107]. An exception is the value for $\hat{\alpha}_4^c$ that is fixed with the polarization data on the $\bar{B} \rightarrow \phi \bar{K}^*$ decay (Eq. (39) in Ref. [107]).

The factorizable coefficients are

$$A_{V_1 V_2}^0 = \frac{f_{V_2}}{f_{K^*}} A_0^{B \rightarrow V_1}(0), \quad A_{V_1 V_2}^\pm = \frac{m_{V_2} f_{V_2}}{m_B f_{K^*}} F_\pm^{B \rightarrow V_1}(0), \tag{128}$$

with $A_0^{B \rightarrow V_1}(0)$ and $F_\pm^{B \rightarrow V_1}(0)$ helicity vector form factors in the definition employed in Ref. [107]. For the $B \rightarrow K^*$ form factors we use the values obtained in Sec. 3.1, whereas for the other transitions we take the values given in that reference. In Table 10, we show the numerical values for the helicity amplitudes for the decays of interest and the respective values for different observables compared with experimental data. The errors are obtained adding linearly those from the input quantities using Monte Carlo techniques.

The contribution of the light resonances to the semileptonic decay amplitudes, in terms of those of the $\bar{B} \rightarrow V \bar{K}^*$ decay, can be expressed as

$$H_{\text{sl},V}^{0,\pm} = \frac{\alpha_{\text{em}} G_F \lambda_t}{\sqrt{2}} \frac{8\pi Q_V f_{K^*} f_V}{(q^2 - m_V^2 + im_V \Gamma_V)} \left(\frac{m_B}{m_V} \right) H_V^{0,\pm}. \tag{129}$$

Notice that the amplitude H_V^+ is completely suppressed in the SM so that the amplitudes $H_V^+(\bar{B} \rightarrow \bar{K}^* \gamma^*)$ in the semileptonic decays are free from this hadronic pollution. On the other hand, and despite of the expected hierarchy in Eq. (126), the results in Table 10 show that numerically $|H_V^-| \sim |H_V^0|$, leading to polarization fractions that are consistent with the experimental values.

Finally, and as explained in Sec. 3.2.3, we make the light-quark contribution calculated in the VMD model to converge to the one obtained in QCDF around $q^2 \simeq 2 \text{ GeV}^2$,

$$\tilde{a}_\mu^{\text{had, lq}} = \tilde{a}_\mu^{\text{had, lq, VMD}} (1 - f(q^2)) + \tilde{a}_\mu^{\text{had, lq, QCDF}} f(q^2), \tag{130}$$

by using the function

$$f(q^2) = \frac{1}{1 + \exp[-a(q^2 - 2)]}. \quad (131)$$

Our numerical results are insensitive to the specific choice of $a > 0$, that we take to be $a = 12$.

References

- [1] R Aaij et al. First evidence for the decay $B_s \rightarrow \mu^+ \mu^-$. 2012, 1211.2674.
- [2] Kristof De Bruyn, Robert Fleischer, Robert Knegjens, Patrick Koppenburg, Marcel Merk, et al. Probing New Physics via the $B_s^0 \rightarrow \mu^+ \mu^-$ Effective Lifetime. *Phys.Rev.Lett.*, 109:041801, 2012, 1204.1737.
- [3] Andrzej J. Buras, Jennifer Girrbach, Diego Guadagnoli, and Gino Isidori. On the Standard Model prediction for $BR(B_{s,d} \rightarrow \mu^+ \mu^-)$. 2012, 1208.0934.
- [4] J. -T. Wei *et al.* [BELLE Collaboration], *Phys. Rev. Lett.* **103** (2009) 171801 [arXiv:0904.0770 [hep-ex]].
- [5] T. Aaltonen *et al.* [CDF Collaboration], *Phys. Rev. Lett.* **106** (2011) 161801 [arXiv:1101.1028 [hep-ex]].
- [6] **LHCb** Collaboration. Differential branching fraction and angular analysis of the $B^0 \rightarrow K^{*0} \ell^+ \ell^-$ decay. LHCb-CONF-2012-008.
- [7] J. L. Ritchie [BABAR Collaboration], arXiv:1301.1700 [hep-ex].
- [8] T. Aaltonen *et al.* [CDF Collaboration], *Phys. Rev. Lett.* **108** (2012) 081807 [arXiv:1108.0695 [hep-ex]].
- [9] B. Aubert *et al.* [BABAR Collaboration], *Phys. Rev. Lett.* **102** (2009) 091803 [arXiv:0807.4119 [hep-ex]].
- [10] J. P. Lees *et al.* [BABAR Collaboration], *Phys. Rev. D* **86** (2012) 032012 [arXiv:1204.3933 [hep-ex]].
- [11] RAaij *et al.* [LHCb Collaboration], *JHEP* **1207** (2012) 133 [arXiv:1205.3422 [hep-ex]].
- [12] T. Aaltonen *et al.* [CDF Collaboration], *Phys. Rev. Lett.* **107** (2011) 201802 [arXiv:1107.3753 [hep-ex]].
- [13] **LHCb** Collaboration, Talk at Moriond 2012, LHCb-CONF-2012-003; P. N. Schaack, CERN-THESIS-2012-064.

- [14] Ahmed Ali, T. Mannel, and T. Morozumi. Forward backward asymmetry of dilepton angular distribution in the decay $b \rightarrow sl^+l^-$. *Phys.Lett.*, B273:505–512, 1991.
- [15] Gustavo Burdman. Short distance coefficients and the vanishing of the lepton asymmetry in $B \rightarrow V\ell^+\ell^-$. *Phys.Rev.*, D57:4254–4257, 1998, hep-ph/9710550.
- [16] D. Melikhov, N. Nikitin, and S. Simula. Probing right-handed currents in $B \rightarrow K^*\ell^+\ell^-$ transitions. *Phys.Lett.*, B442:381–389, 1998, hep-ph/9807464.
- [17] Ahmed Ali, Patricia Ball, L.T. Handoko, and G. Hiller. A Comparative study of the decays $B \rightarrow (K, K^*)\ell^+\ell^-$ in standard model and supersymmetric theories. *Phys.Rev.*, D61:074024, 2000, hep-ph/9910221.
- [18] Frank Kruger, Lalit M. Sehgal, Nita Sinha, and Rahul Sinha. Angular distribution and CP asymmetries in the decays $\bar{B} \rightarrow K^-\pi^+e^-e^+$ and $\bar{B} \rightarrow \pi^-\pi^+e^-e^+$. *Phys.Rev.*, D61:114028, 2000, hep-ph/9907386.
- [19] C.S. Kim, Yeong Gyun Kim, Cai-Dian Lu, and Takuya Morozumi. Azimuthal angle distribution in $B \rightarrow K^*(\rightarrow K\pi)\ell^+\ell^-$ at low invariant $m(\ell^+\ell^-)$ region. *Phys.Rev.*, D62:034013, 2000, hep-ph/0001151.
- [20] Gustavo Burdman and Gudrun Hiller. Semileptonic form-factors from $B \rightarrow K^*\gamma$ decays in the large energy limit. *Phys.Rev.*, D63:113008, 2001, hep-ph/0011266.
- [21] Yuval Grossman and Dan Pirjol. Extracting and using photon polarization information in radiative B decays. *JHEP*, 0006:029, 2000, hep-ph/0005069.
- [22] C.S. Kim, Yeong Gyun Kim, and Cai-Dian Lu. Possible supersymmetric effects on angular distributions in $B \rightarrow K^*(\rightarrow K\pi)\ell^+\ell^-$ decays. *Phys.Rev.*, D64:094014, 2001, hep-ph/0102168.
- [23] M. Beneke, T. Feldmann, and D. Seidel. Systematic approach to exclusive $B \rightarrow V\ell^+\ell^-, V\gamma$ decays. *Nucl.Phys.*, B612:25–58, 2001, hep-ph/0106067.
- [24] Stefan W. Bosch and Gerhard Buchalla. The Radiative decays $B \rightarrow V\gamma$ at next-to-leading order in QCD. *Nucl.Phys.*, B621:459–478, 2002, hep-ph/0106081.
- [25] Ahmed Ali and A. Salim Safir. Helicity analysis of the decays $B \rightarrow K^*\ell^+\ell^-$ and $B \rightarrow \rho\ell^+\ell^-$ in the large energy effective theory. *Eur.Phys.J.*, C25:583–601, 2002, hep-ph/0205254.

- [26] Amand Faessler, T. Gutsche, M.A. Ivanov, J.G. Korner, and Valery E. Lyubovitskij. The Exclusive rare decays $B \rightarrow K(K^*)\bar{\ell}\ell$ and $B_c \rightarrow D(D^*)\bar{\ell}\ell$ in a relativistic quark model. *Eur.Phys.J.direct*, C4:18, 2002, hep-ph/0205287.
- [27] Alexander L. Kagan and Matthias Neubert. Isospin breaking in $B \rightarrow K^* \gamma$ decays. *Phys.Lett.*, B539:227–234, 2002, hep-ph/0110078.
- [28] Thorsten Feldmann and Joaquim Matias. Forward-backward and isospin asymmetry for $B \rightarrow K^*l^+l^-$ decay in the standard model and in supersymmetry. *JHEP*, 0301:074, 2003, hep-ph/0212158.
- [29] M. Beneke, Th. Feldmann, and D. Seidel. Exclusive radiative and electroweak $b \rightarrow d$ and $b \rightarrow s$ penguin decays at NLO. *Eur.Phys.J.*, C41:173–188, 2005, hep-ph/0412400.
- [30] Benjamin Grinstein and Dan Pirjol. Exclusive rare $B \rightarrow K^*\ell^+\ell^-$ decays at low recoil: Controlling the long-distance effects. *Phys.Rev.*, D70:114005, 2004, hep-ph/0404250.
- [31] Benjamin Grinstein and Dan Pirjol. Factorization in $B \rightarrow K\pi l^+l^-$ decays. *Phys.Rev.*, D73:094027, 2006, hep-ph/0505155.
- [32] Frank Kruger and Joaquim Matias. Probing new physics via the transverse amplitudes of $B^0 \rightarrow K^{*0}(\rightarrow K^-\pi^+)\ell^+\ell^-$ at large recoil. *Phys.Rev.*, D71:094009, 2005, hep-ph/0502060.
- [33] Joaquim Matias. The Angular distribution of $B^0 \rightarrow K^{*0}(\rightarrow K^-\pi^+)\ell^+\ell^-$ at large recoil in and beyond the SM. *PoS*, HEP2005:281, 2006, hep-ph/0511274.
- [34] Patricia Ball and Roman Zwicky. Time-dependent CP Asymmetry in $B \rightarrow K^*\gamma$ as a (Quasi) Null Test of the Standard Model. *Phys.Lett.*, B642:478–486, 2006, hep-ph/0609037.
- [35] Patricia Ball, Gareth W. Jones, and Roman Zwicky. $B \rightarrow V\gamma$ beyond QCD factorisation. *Phys.Rev.*, D75:054004, 2007, hep-ph/0612081.
- [36] E. Lunghi and J. Matias. Huge right-handed current effects in $B \rightarrow K^*(K\pi)\ell^+\ell^-$ in supersymmetry. *JHEP*, 0704:058, 2007, hep-ph/0612166.
- [37] Christoph Bobeth, Gudrun Hiller, and Giorgi Piranishvili. CP Asymmetries in $\bar{B} \rightarrow \bar{K}^*(\rightarrow \bar{K}\pi)\bar{\ell}\ell$ and Untagged $\bar{B}_s, B_s \rightarrow \phi(\rightarrow K^+K^-)\bar{\ell}\ell$ Decays at NLO. *JHEP*, 0807:106, 2008, 0805.2525.
- [38] U. Egede, T. Hurth, J. Matias, M. Ramon, and W. Reece. New observables in the decay mode $\bar{B} \rightarrow \bar{K}^{*0}l^+l^-$. *JHEP*, 0811:032, 2008, 0807.2589.

- [39] Wolfgang Altmannshofer, Patricia Ball, Aoife Bharucha, Andrzej J. Buras, David M. Straub, et al. Symmetries and Asymmetries of $B \rightarrow K^* \mu^+ \mu^-$ Decays in the Standard Model and Beyond. *JHEP*, 0901:019, 2009, 0811.1214.
- [40] U. Egede, T. Hurth, J. Matias, M. Ramon, and W. Reece. The exclusive $B \rightarrow K^*(\rightarrow K\pi)l^+l^-$ decay: CP conserving observables. *Acta Phys.Polon.*, B3:151–157, 2010, 0912.1339.
- [41] Ulrik Egede, Tobias Hurth, Joaquim Matias, Marc Ramon, and Will Reece. New physics reach of CP violating observables in the decay $B \rightarrow K^*l^+l^-$. *PoS*, EPS-HEP2009:184, 2009, 0912.1349.
- [42] Christoph Bobeth, Gudrun Hiller, and Danny van Dyk. The Benefits of $\bar{B} \rightarrow \bar{K}^*l^+l^-$ Decays at Low Recoil. *JHEP*, 1007:098, 2010, 1006.5013.
- [43] Aoife Bharucha and William Reece. Constraining new physics with $B \rightarrow K^* \mu^+ \mu^-$ in the early LHC era. *Eur.Phys.J.*, C69:623–640, 2010, 1002.4310.
- [44] Ashutosh Kumar Alok, Amol Dighe, Diptimoy Ghosh, David London, Joaquim Matias, et al. New-physics contributions to the forward-backward asymmetry in $B \rightarrow K^* \mu^+ \mu^-$. *JHEP*, 1002:053, 2010, 0912.1382.
- [45] Ulrik Egede, Tobias Hurth, Joaquim Matias, Marc Ramon, and Will Reece. New physics reach of the decay mode $\bar{B} \rightarrow \bar{K}^{*0} \ell^+ \ell^-$. *JHEP*, 1010:056, 2010, 1005.0571.
- [46] A. Khodjamirian, Th. Mannel, A.A. Pivovarov, and Y.-M. Wang. Charm-loop effect in $B \rightarrow K^{(*)} \ell^+ \ell^-$ and $B \rightarrow K^* \gamma$. *JHEP*, 1009:089, 2010, 1006.4945.
- [47] Ashutosh Kumar Alok, Alakabha Datta, Amol Dighe, Murugeswaran Duraisamy, Diptimoy Ghosh, et al. New Physics in $b \rightarrow s \mu^+ \mu^-$: CP-Conserving Observables. 2010, 1008.2367.
- [48] E. Kou, A. Le Yaouanc, and A. Tayduganov. Determining the photon polarization of the $b \rightarrow s \gamma$ using the $B \rightarrow K_1(1270) \gamma \rightarrow (K \pi \pi) \gamma$ decay. *Phys.Rev.*, D83:094007, 2011, 1011.6593.
- [49] Qin Chang, Xin-Qiang Li, and Ya-Dong Yang. $B \rightarrow K^*l^+l^-, Kl^+l^-$ decays in a family non-universal Z' model. *JHEP*, 1004:052, 2010, 1002.2758.
- [50] W. R. Reece. Exploiting angular correlations in the rare decay $B \rightarrow K^* \mu^+ \mu^-$ at LHCb. *CERN-THESIS-2010-095*, 2010.
- [51] M. Beylich, G. Buchalla, and Th. Feldmann. Theory of $B \rightarrow K^{(*)}l^+l^-$ decays at high q^2 : OPE and quark-hadron duality. *Eur.Phys.J.*, C71:1635, 2011, 1101.5118. * Temporary entry *

- [52] Christoph Bobeth, Gudrun Hiller, and Danny van Dyk. More Benefits of Semileptonic Rare B Decays at Low Recoil: CP Violation. 2011, 1105.0376. * Temporary entry *.
- [53] Damir Becirevic and Elia Schneider. On transverse asymmetries in $B \rightarrow K^*l^+l^-$. *Nucl.Phys.*, B854:321–339, 2012, 1106.3283.
- [54] Ashutosh Kumar Alok, Alakabha Datta, Amol Dighe, Murugeswaran Duraisamy, Diptimoy Ghosh, et al. New Physics in $b \rightarrow s\mu^+\mu^-$: CP-Violating Observables. *JHEP*, 1111:122, 2011, 1103.5344.
- [55] Cai-Dian Lu and Wei Wang. Analysis of $B \rightarrow K_J^*(\rightarrow K\pi)\mu^+\mu^-$ in the higher kaon resonance region. *Phys.Rev.*, D85:034014, 2012, 1111.1513.
- [56] Ru-Min Wang, Yuan-Guo Xu, Yi-Long Wang, and Ya-Dong Yang. Revisiting $B_s \rightarrow \mu^+\mu^-$ and $B \rightarrow K^{(*)}\mu^+\mu^-$ decays in the MSSM with and without R-parity. *Phys.Rev.*, D85:094004, 2012, 1112.3174.
- [57] Joaquim Matias, Federico Mescia, Marc Ramon, and Javier Virto. Complete Anatomy of $\bar{B}_d \rightarrow \bar{K}^{*0}(\rightarrow K\pi)l^+l^-$ and its angular distribution. *JHEP*, 1204:104, 2012, 1202.4266.
- [58] Damir Becirevic and Andrey Tayduganov. Impact of $B \rightarrow K_0^*\ell^+\ell^-$ on the New Physics search in $B \rightarrow K^*\ell^+\ell^-$ decay. 2012, 1207.4004.
- [59] Alexander Yu. Korchin and Vladimir A. Kovalchuk. Contribution of vector resonances to the $\bar{B}_d^0 \rightarrow \bar{K}^{*0}\mu^+\mu^-$ decay. *Eur.Phys.J.*, C72:2155, 2012, 1205.3683.
- [60] Diganta Das and Rahul Sinha. New Physics Effects and Hadronic Form Factor Uncertainties in $B \rightarrow K^*\ell^+\ell^-$. *Phys.Rev.*, D86:056006, 2012, 1205.1438.
- [61] Joaquim Matias. On the S-wave pollution of $B \rightarrow K^*l^+l^-$ observables. 2012, 1209.1525.
- [62] Thomas Blake, Ulrik Egede, and Alex Shires. The effect of S-wave interference on the $B^0 \rightarrow K^{*0}\ell^+\ell^-$ angular observables. 2012, 1210.5279.
- [63] Wolfgang Altmannshofer, Paride Paradisi, and David M. Straub. Model-Independent Constraints on New Physics in $b \rightarrow s$ Transitions. *JHEP*, 1204:008, 2012, 1111.1257.
- [64] Sebastien Descotes-Genon, Diptimoy Ghosh, Joaquim Matias, and Marc Ramon. Exploring New Physics in the $C_7 - C_7'$ plane. *JHEP*, 1106:099, 2011, 1104.3342.

- [65] Frederik Beaujean, Christoph Bobeth, Danny van Dyk, and Christian Wacker. Bayesian Fit of Exclusive $b \rightarrow s\bar{\ell}\ell$ Decays: The Standard Model Operator Basis. *JHEP*, 1208:030, 2012, 1205.1838.
- [66] Sebastien Descotes-Genon, Joaquim Matias, Marc Ramon, and Javier Virto. Implications from clean observables for the binned analysis of $B \rightarrow K^*l\bar{l}$ at large recoil. 2012, 1207.2753.
- [67] Wolfgang Altmannshofer and David M. Straub. Cornering New Physics in $b \rightarrow s$ Transitions. *JHEP*, 1208:121, 2012, 1206.0273.
- [68] Arnd Behring, Christian Gross, Gudrun Hiller, and Stefan Schacht. Squark Flavor Implications from $B \rightarrow K^*\ell^+\ell^-$. *JHEP*, 1208:152, 2012, 1205.1500.
- [69] Patricia Ball and Vladimir M. Braun. Exclusive semileptonic and rare B meson decays in QCD. *Phys.Rev.*, D58:094016, 1998, hep-ph/9805422.
- [70] J. Charles, A. Le Yaouanc, L. Oliver, O. Pene, and J.C. Raynal. Heavy to light form-factors in the heavy mass to large energy limit of QCD. *Phys.Rev.*, D60:014001, 1999, hep-ph/9812358.
- [71] M. Beneke and T. Feldmann. Symmetry breaking corrections to heavy to light B meson form-factors at large recoil. *Nucl.Phys.*, B592:3–34, 2001, hep-ph/0008255.
- [72] Damir Becirevic, Emi Kou, Alain Le Yaouanc, and Andrey Tayduganov. Future prospects for the determination of the Wilson coefficient $C'_{7\gamma}$. *JHEP*, 1208:090, 2012, 1206.1502.
- [73] Konstantin G. Chetyrkin, Mikolaj Misiak, and Manfred Munz. Weak radiative B meson decay beyond leading logarithms. *Phys.Lett.*, B400:206–219, 1997, hep-ph/9612313.
- [74] Aoife Bharucha, Thorsten Feldmann, and Michael Wick. Theoretical and Phenomenological Constraints on Form Factors for Radiative and Semi-Leptonic B -Meson Decays. *JHEP*, 1009:090, 2010, 1004.3249.
- [75] Damir Becirevic, Vittorio Lubicz, and Federico Mescia. An Estimate of the $B \rightarrow K^*\gamma$ form factor. *Nucl.Phys.*, B769:31–43, 2007, hep-ph/0611295.
- [76] Zhaofeng Liu, Stefan Meinel, Alistair Hart, Ron R. Horgan, Eike H. Muller, et al. A Lattice calculation of $B \rightarrow K^{(*)}$ form factors. 2011, 1101.2726.
- [77] Patricia Ball and Roman Zwicky. $B_{d,s} \rightarrow \rho, \omega, K^*, \phi$ decay form-factors from light-cone sum rules revisited. *Phys.Rev.*, D71:014029, 2005, hep-ph/0412079.

- [78] Christian W. Bauer, Sean Fleming, Dan Pirjol, and Iain W. Stewart. An Effective field theory for collinear and soft gluons: Heavy to light decays. *Phys.Rev.*, D63:114020, 2001, hep-ph/0011336.
- [79] Christian W. Bauer, Dan Pirjol, and Iain W. Stewart. Soft collinear factorization in effective field theory. *Phys.Rev.*, D65:054022, 2002, hep-ph/0109045.
- [80] M. Beneke, A.P. Chapovsky, M. Diehl, and T. Feldmann. Soft collinear effective theory and heavy to light currents beyond leading power. *Nucl.Phys.*, B643:431–476, 2002, hep-ph/0206152.
- [81] M. Beneke and T. Feldmann. Multipole expanded soft collinear effective theory with nonAbelian gauge symmetry. *Phys.Lett.*, B553:267–276, 2003, hep-ph/0211358.
- [82] M. Beneke and T. Feldmann. Factorization of heavy to light form-factors in soft collinear effective theory. *Nucl.Phys.*, B685:249–296, 2004, hep-ph/0311335.
- [83] M. Beneke and D. Yang. Heavy-to-light B meson form-factors at large recoil energy: Spectator-scattering corrections. *Nucl.Phys.*, B736:34–81, 2006, hep-ph/0508250.
- [84] M. Beneke, Y. Kiyo, and D.s. Yang. Loop corrections to subleading heavy quark currents in SCET. *Nucl.Phys.*, B692:232–248, 2004, hep-ph/0402241.
- [85] Thomas Becher and Richard J. Hill. Loop corrections to heavy-to-light form-factors and evanescent operators in SCET. *JHEP*, 0410:055, 2004, hep-ph/0408344.
- [86] G.G. Kirilin. Loop corrections to the form-factors in $B \rightarrow \pi l \nu$ decay. 2005, hep-ph/0508235.
- [87] P. Colangelo, F. De Fazio, Pietro Santorelli, and E. Scrimieri. QCD sum rule analysis of the decays $B \rightarrow K l^+ l^-$ and $B \rightarrow K^* l^+ l^-$. *Phys.Rev.*, D53:3672–3686, 1996, hep-ph/9510403.
- [88] Mikhail A. Ivanov, Jurgen G. Korner, Sergey G. Kovalenko, and Craig D. Roberts. B to light-meson transition form-factors. *Phys.Rev.*, D76:034018, 2007, nucl-th/0703094.
- [89] E. Bagan, Patricia Ball, and Vladimir M. Braun. Radiative corrections to the decay $B \rightarrow \pi e \nu$ and the heavy quark limit. *Phys.Lett.*, B417:154–162, 1998, hep-ph/9709243.

- [90] T. Feldmann. Talk at Workshop on the Physics Reach of Rare and Exclusive semileptonic B decays, University of Sussex, September 10-11, 2012.
- [91] M. Beneke, G. Buchalla, M. Neubert, and Christopher T. Sachrajda. QCD factorization in $B \rightarrow \pi K, \pi\pi$ decays and extraction of Wolfenstein parameters. *Nucl.Phys.*, B606:245–321, 2001, hep-ph/0104110.
- [92] M.B. Voloshin. Large $\mathcal{O}(m_c^{-2})$ nonperturbative correction to the inclusive rate of the decay $B \rightarrow X_s \gamma$. *Phys.Lett.*, B397:275–278, 1997, hep-ph/9612483.
- [93] Zoltan Ligeti, Lisa Randall, and Mark B. Wise. Comment on nonperturbative effects in $\bar{B} \rightarrow X_s \gamma$. *Phys.Lett.*, B402:178–182, 1997, hep-ph/9702322.
- [94] A. Khodjamirian, Th. Mannel, and Y.-M. Wang. $B \rightarrow K \ell^+ \ell^-$ decay at large hadronic recoil. 2012, 1211.0234.
- [95] Steven Weinberg. Phenomenological Lagrangians. *Physica*, A96:327, 1979.
- [96] J. Gasser and H. Leutwyler. Chiral Perturbation Theory to One Loop. *Annals Phys.*, 158:142, 1984.
- [97] G. Ecker, J. Gasser, A. Pich, and E. de Rafael. The Role of Resonances in Chiral Perturbation Theory. *Nucl.Phys.*, B321:311, 1989.
- [98] G. Ecker, J. Gasser, H. Leutwyler, A. Pich, and E. de Rafael. Chiral Lagrangians for Massive Spin 1 Fields. *Phys.Lett.*, B223:425, 1989.
- [99] J.A. Oller, E. Oset, and J.R. Pelaez. Meson meson interaction in a nonperturbative chiral approach. *Phys.Rev.*, D59:074001, 1999, hep-ph/9804209.
- [100] J.A. Oller and E. Oset. N/D description of two meson amplitudes and chiral symmetry. *Phys.Rev.*, D60:074023, 1999, hep-ph/9809337.
- [101] Vincenzo Cirigliano, Gerhard Ecker, Helmut Neufeld, Antonio Pich, and Jorge Portoles. Kaon Decays in the Standard Model. *Rev.Mod.Phys.*, 84:399, 2012, 1107.6001.
- [102] Johan Bijnens and Ilaria Jemos. Hard Pion Chiral Perturbation Theory for $B \rightarrow \pi$ and $D \rightarrow \pi$ Formfactors. *Nucl.Phys.*, B840:54–66, 2010, 1006.1197.
- [103] Gilberto Colangelo, Massimiliano Procura, Lorena Rothen, Ramon Stucki, and Jaume Tarrus. On the factorization of chiral logarithms in the pion form factors. 2012, 1208.0498.
- [104] Gerard 't Hooft. A Planar Diagram Theory for Strong Interactions. *Nucl.Phys.*, B72:461, 1974.

- [105] Peter Lichard. Some implications of meson dominance in weak interactions. *Phys.Rev.*, D55:5385–5407, 1997, hep-ph/9702345.
- [106] Alexander Yu. Korchin and Vladimir A. Kovalchuk. Asymmetries in $\bar{B}_d^0 \rightarrow \bar{K}^{*0} e^+ e^-$ decay and contribution of vector resonances. 2011, 1111.4093.
- [107] Martin Beneke, Johannes Rohrer, and Deshan Yang. Branching fractions, polarisation and asymmetries of $B \rightarrow VV$ decays. *Nucl.Phys.*, B774:64–101, 2007, hep-ph/0612290.
- [108] Alexander L. Kagan. Polarization in $B \rightarrow VV$ decays. *Phys.Lett.*, B601:151–163, 2004, hep-ph/0405134.
- [109] Bernard Aubert et al. Measurement of the $B^0 \rightarrow \phi K^0$ decay amplitudes. *Phys.Rev.Lett.*, 93:231804, 2004, hep-ex/0408017.
- [110] K.-F. Chen et al. Measurement of polarization and triple-product correlations in $B \rightarrow \phi K^*$ decays. *Phys.Rev.Lett.*, 94:221804, 2005, hep-ex/0503013.
- [111] N. Serra. Private communication.
- [112] Joaquim Matias, S. Descotes-Genon, and Javier Virto. To appear.
- [113] R Aaij et al. Measurement of the CP asymmetry in $B^0 \rightarrow K^{*0} \mu^+ \mu^-$ decays. 2012, 1210.4492.
- [114] J. Lefrançois and M.H. Schune. Measuring the photon polarization in $b \rightarrow s\gamma$ using the $B \rightarrow K^* e^+ e^-$ decay channel. 2009.
- [115] M. Jacob and G.C. Wick. On the general theory of collisions for particles with spin. *Annals Phys.*, 7:404–428, 1959.
- [116] J. Charles et al. CP violation and the CKM matrix: Assessing the impact of the asymmetric B factories. *Eur.Phys.J.*, C41:1–131, 2005, hep-ph/0406184.
- [117] K. Nakamura et al. Review of particle physics. *J.Phys.G*, G37:075021, 2010.
- [118] Gilberto Colangelo, Stephan Durr, Andreas Juttner, Laurent Lellouch, Heinrich Leutwyler, et al. Review of lattice results concerning low energy particle physics. *Eur.Phys.J.*, C71:1695, 2011, 1011.4408.
- [119] K.G. Chetyrkin, Johann H. Kuhn, and M. Steinhauser. RunDec: A Mathematica package for running and decoupling of the strong coupling and quark masses. *Comput.Phys.Commun.*, 133:43–65, 2000, hep-ph/0004189.

- [120] Heechang Na, Chris J. Monahan, Christine T.H. Davies, Ron Horgan, G. Peter Lepage, et al. The B and B_s Meson Decay Constants from Lattice QCD. *Phys.Rev.*, D86:034506, 2012, 1202.4914.
- [121] Y. Amhis et al. Averages of b -hadron, c -hadron, and τ -lepton properties as of early 2012. 2012, 1207.1158.
- [122] M. Dimou, J. Lyon and R. Zwicky, arXiv:1212.2242 [hep-ph].
- [123] C. Bobeth, G. Hiller and D. van Dyk, arXiv:1212.2321 [hep-ph].